

~~CONFIDENTIAL~~

Copy 6
RM E55F08

NACA RM E55F08

NACA

RESEARCH MEMORANDUM

PERFORMANCE OF INCONEL 550 TURBINE BLADES
IN A TURBOJET ENGINE AND EFFECTS OF
DIFFERENT FORGING TEMPERATURES
AND HEAT TREATMENTS

By C. A. Gyorgak, J. R. Johnston, and J. W. Weeton

Lewis Flight Propulsion Laboratory
CLASSIFICATION CHANGED Cleveland, Ohio

UNCLASSIFIED

Authority of *NACA Reels*
42N 116 Date *June 20, 1957*
CLASSIFIED DOCUMENT

627857

This material contains information affecting the National Defense of the United States within the meaning of the espionage laws, Title 18, U.S.C., Secs. 793 and 794, the transmission or revelation of which in any manner to an unauthorized person is prohibited by law.

**NATIONAL ADVISORY COMMITTEE
FOR AERONAUTICS**

WASHINGTON

August 16, 1955

~~CONFIDENTIAL~~



NATIONAL ADVISORY COMMITTEE FOR AERONAUTICS

RESEARCH MEMORANDUM

PERFORMANCE OF INCONEL 550 TURBINE BLADES IN A TURBOJET

ENGINE AND EFFECTS OF DIFFERENT FORGING

TEMPERATURES AND HEAT TREATMENTS

By C. A. Gyorgak, J. R. Johnston, and J. W. Weeton

SUMMARY

An investigation was conducted to determine the effects of forging at 1950° and 2150° F as well as the effects of several heat treatments upon the performance of Inconel 550 in a turbojet engine. The turbine blades were operated at a nominal temperature of 1500° F and a centrifugal stress within the critical zone of the blade airfoil of 19,200 psi. The engine was operated in a cyclic manner for 15 minutes at rated and 5 minutes at idle speed.

The engine lives of the best-performing group of blades varied from 450 to 857 hours, whereas lives of Air Force stock S-816 blades used as a standard ranged from 204 to 599 hours.

Differences in engine performance of the various groups of Inconel 550 turbine blades could not be associated with consistent differences in microstructure or grain size. The best-performing group of blades had larger grains than the other groups of blades and a wider range of grain sizes, even though fatigue was associated with the failures.

INTRODUCTION

Inconel 550 is a potential turbine-blade material having a low strategic-element content relative to the extensively used blade alloy S-816. Essentially, Inconel 550 is a modification of precipitation-hardening Inconel X in that the aluminum is increased from 0.7 to 1.2 percent (ref. 1). The published stress-rupture properties of Inconel 550 are approximately equivalent to the values shown in the upper portion of the scatter band for Inconel X (ref. 2).

The investigation reported herein was conducted at the NACA Lewis laboratory to determine the effects upon blade performance of (1) blade forging temperatures of 1950° and 2150° F and (2) several heat treatments. It was also desired to correlate blade performance with the expected difference in grain size associated with varying forging temperature and heat treatment.

Blade performance was determined in an engine under cyclic operating conditions. The stress-rupture lives of specimens cut from blade airfoils were determined at a temperature of 1500° F under stresses of 20,000, 25,000, or 30,000 psi and were compared with data obtained from bar stock of the same heat.

Metallurgical studies were made of blades in the as-heat-treated and in the engine-operated conditions. An attempt was made to relate microstructure, grain size, and hardness to blade performance.

MATERIALS, APPARATUS, AND PROCEDURE

Turbine Blades

The chemical composition of the blades studied (ref. 2) is as follows:

C	Mn	Fe	Si	S	Cu	Cr	Al	Ti	Cb and Ta	Ni
0.05	0.73	6.59	0.28	0.007	0.03	14.97	1.16	2.15	1.03	^a 72.65

^aBy difference.

The blades were precision forged from a single heat of alloy. Forging temperatures and heat treatments are listed in table I. Seven blades of each Inconel 550 group (table I) and eight S-816 blades selected from stock as standards of comparison were chosen by random numbers for evaluation in the engine and inserted randomly in a wheel. All blades used in this investigation passed both X-ray and zygo inspection specifications.

Engine Operation

The 50 blades selected for engine tests were run to failure in a J33-9 engine under cyclic conditions. Cycles were of 20-minute duration and consisted of 15 minutes at the rated speed of 11,500 rpm and approximately 5 minutes at an idle speed of 4000 rpm.

Engine operation was interrupted to obtain data on blade elongation, to check blades for cracks, to replace failed blades, to overhaul the engine when necessary, and at the end of each 8-hour workday.

Stress and temperature distribution in turbine blades during engine operation. - The cross sections of two as-received Inconel 550 blades were measured with an optical comparator to permit calculation of the centrifugal-stress distribution along the blade length (ref. 3).

Blade temperatures during rated speed were measured on four thermocoupled S-816 blades placed at 90° intervals around the wheel. Temperatures were recorded by an electronic potentiometer.

Figure 1 shows the results of a temperature survey made during the initial stages of engine operation. The three temperature points do not in themselves completely define the curve; however, this curve has been drawn to correspond to the shape of curves obtained from previous temperature surveys in this engine.

The stress-rupture life of the alloy corresponding to the conditions of centrifugal stress and temperature at different sections of the airfoil is also shown in figure 1. These curves were constructed using data for blade airfoil specimens (table II) and manufacturer's data. Several different extrapolation procedures were used. The results obtained for the minimum stress-rupture life were very similar because this extrapolation was limited to small differences in stress and temperature. If the failures result solely from the most severe combination of stress and temperature, blades would be expected to fail in a "critical zone" with operating lives approximately equal to the minimums of the stress-rupture-life curves.

Blade-elongation measurements. - Two blades of each group were scribed at 1/2-inch intervals, as shown in figure 2. Elongation measurements were made at approximately 10-hour intervals for the first 50 hours of test time and at approximately 35-hour intervals for the remainder of the test life. The elongation of each scribed segment was measured with an optical extensometer having a sensitivity of 0.001 inch. Accuracy of the elongation measurements is, however, influenced by the degree of blade distortion and warpage.

Macroexamination of blades. - Two blades from group 4 and six blades from each of the other groups were macroetched in a solution of 80 percent hydrochloric acid and 20 percent hydrogen peroxide to reveal grain size and flow lines. These blades were also used for macro- and microstudies and stress-rupture tests.

The blades, which were visually inspected before being placed in the engine, were also inspected for cracks at intervals throughout the engine-operation phase of the investigation.

A blade was considered to have failed either when actual fracture occurred or when cracks in the airfoil made it apparent that failure was imminent. Failed blades were examined at low magnification to determine the type of failure. In addition, macroetching was employed to reveal grain size and to differentiate between intercrystalline and transcrystalline cracking. Failures may be classified in the following manner:

(1) Stress-rupture - Blade failure occurred by cracking within the airfoil or by fracturing in an irregular, jagged, intercrystalline path. Other similar cracks sometimes occurred near the origin of the main fracture.

(2) Fatigue - Cracks progressed from nucleation sites, usually at or near the leading or trailing edges, in straight paths, which frequently were smooth; they often showed progression lines or concentric rings and appeared to be transcrystalline.

(3) Stress-rupture followed by fatigue - Blade failures appeared to be caused by a combination of the two preceding mechanisms. The fracture surface consisted of a small area having characteristics of stress-rupture and a larger area with fatigue characteristics. A further criterion was the appearance of secondary stress-rupture cracks near the nucleation site of the main crack.

(4) Damage - Blades showing nicks or dents in the airfoil which might possibly initiate fracture were not considered in the analysis of the data, since they do not yield a true indication of material properties.

A basic difficulty in defining the failure mechanism from the appearance of the fracture surface alone is that the effect of superimposed fatigue damage is not always evident. In reference 4, for example, the high-temperature life was determined for specimens subjected to vibratory loads superimposed upon constant loads. In many cases the fracture surface of the specimens showed no evidence of fatigue damage, although reduction in life was caused by the superimposed vibratory loads.

Metallographic Examination

Heat-treated blades. - Two blades of each group were sectioned approximately $2\frac{13}{16}$ inches above the base after heat treatment for metallographic examination.

Failed blades. - First and last failed blades of each group were sectioned to include the failure origin. The reported metallographic examinations for microstructure and grain size were made on these longitudinal (spanwise) sections.

Hardness Determinations

Four hardness readings were made on the metallographic specimens of the heat-treated blades. Hardness values for failed blades were made on cross sections approximately 1/4 inch below the failure origin.

Stress-Rupture Tests

Stress-rupture specimens were machined from the airfoil as shown in figure 3. Specimens of each group were tested at stress levels of 20,000, 25,000, and 30,000 psi at 1500° F.

The data obtained from these tests were compared with the engine life of the alloy and the stress-rupture life of bar-stock specimens given the same heat treatment as the blades of group 1.

RESULTS

Blade Performance

The engine lives for the different groups of blades are shown in figure 4 and are listed in table III. The best performance was obtained from blades of group 1 forged at 2150° F, solution treated at 2150° F, aged at 1600° and 1350° F. The life of this group was about double that of standard S-816.

Blade performances of groups 4 to 6 were about equal and were about 1.6 times the life of the standard S-816 group.

Blade performances of groups 2 and 3 were essentially equal to the performance of standard S-816.

Time to first failure for all the Inconel 550 alloy groups was greater than that for S-816 blades, with the exception of the blades of group 2, which had a first-failure time almost equivalent to that of the S-816 blades.

Blade Elongation During Engine Operation

Elongation of Inconel 550 and S-816 blades is shown in figure 5 as a function of operating time. The total measured elongations of Inconel 550 blades were essentially the same for each heat-treated group and less than 0.3 percent in the zone of greatest creep (positions 2 and 3, $1\frac{1}{2}$ to $2\frac{1}{2}$ in., respectively, above the base). The elongation of S-816 blades in the same zone was as high as 9 percent. Elongation of the Inconel 550 in sections above and below the zone of greatest creep was too small to determine.

Microstructure of As-Heat-Treated Blades

In precipitation-hardening alloys, the amount of precipitate within the matrix of the alloy usually depends upon the heat treatment. However, in the blades of Inconel 550, the quantity of general precipitation (visible after etching) appeared to be the same for all heat treatments used in this investigation. Furthermore, the variations in matrix precipitation were as great from section to section within single blades as variations from one group of blades to another. The microstructure shown in figure 6 may be considered typical of the majority of blades. Other types of microstructure can be seen in figure 7. Figure 7(a) shows a lamellar precipitate, which occurred in the leading and trailing edges of a few blades of each group.

Also, at the leading and trailing edges of blades from all groups, various degrees of slip-plane precipitation were noted (fig. 7(b)). These precipitations at the blade edges indicate that cold-working occurred during forging.

Depletion zones not connected with surface phenomena occurred along a few grain boundaries in a majority of the Inconel 550 groups. The largest zone detected is shown in figure 7(c).

The photomicrograph of figure 7(d) shows an example of a thick segregation of precipitates in a grain boundary. The greatest quantity of this type of grain-boundary precipitate that was noted in the different groups of alloys is shown in figure 7(e).

Grain Size

Photographs of macroetched blades are shown in figure 8. Where no variation in grain size was noted within a blade group, only one blade was photographed; however, where a variation existed, extreme differences are shown.

Generally, regions near the base and the central longitudinal sections contained the largest grains. In some cases, large grains also appeared in the leading and trailing edges.

The largest grains and the greatest scatter in grain size on a macrobasis were noted in the best-performing group of blades (group 1), which was expected to contain uniform, medium-sized grains.

The group of blades that was expected to contain the largest grains, group 6, had a mixed grain size, but the range in size was considered to be less than that occurring in group 1. The remaining four groups had approximately uniform and "fine" grains.

Grain-size measurements made on cross sections $2\frac{13}{16}$ inches from the blade base are shown in table IV and figure 9. Both coarse and very fine grains were observed in almost all the specimens. These sections are not necessarily representative of the grain sizes of the entire airfoil. Therefore, the macroetched blades are considered to give a better indication of relative grain sizes.

Metallurgical Studies of Failed Blades

Of the six groups tested, all first failures occurred by fatigue, five of them occurring in the leading edge approximately 3 inches above the base and the other originating in the trailing edge, also approximately 3 inches above the base. The last failures occurred as follows: two by fatigue, one by stress rupture followed by fatigue, and three by stress rupture. Failures from fatigue and from stress rupture followed by fatigue originated in the leading edge, high in the airfoil, while the stress-rupture failures originated away from the leading or trailing edge of the blade and occurred within the critical zone.

Photomicrographs of failure origins of first and last blade failures for each group are shown in figure 10. No definite microstructural differences were noted between first and last failures even though the difference in life was as great as 469 hours. The only definite difference between the microstructures of heat-treated and operated blades was that the operated blades etched more rapidly. All specimens examined had depletion zones and showed some oxide penetration of the grain

boundaries. Failures appeared to initiate at oxide penetrations and recrystallization occurred in the surface grains of some blades. A typical microstructure of operated blades is shown in figure 11.

Stress-Rupture Tests

The stress-rupture lives of specimens cut from blade airfoils are given in table II. These values are also plotted in figure 12 along with the stress-rupture strength of bar stock given the same heat treatment as group 1. Blade-life values of the different groups are also plotted in figure 12 at stress levels corresponding to the centrifugal stresses at the failure origins in the blade airfoils. Reasons for plotting in this manner will be discussed later.

The average stress-rupture life at 1500° F and 20,000 psi (table II) of groups 1 and 4 is 740 hours and is approximately equivalent to that of bar stock given the same heat treatment as group 1. The average stress-rupture life at 1500° F and 20,000 psi of each of the other four groups (2, 3, 5, and 6) was practically the same and approximately 250 hours less than the bar-stock life or lives of groups 1 and 4.

Hardness

The Rockwell hardness values of heat-treated and of failed blades are shown in table V. It should be again mentioned that the hardness readings on the failed blades were made 1/4 inch below the fracture edges and that these readings may not have been typical of the entire blade.

Hardness of heat-treated blades was lowest (Rockwell C-22) for blades of group 6, which were solution treated the longest time at the highest temperature (4 hr at 2150° F). The highest hardness (Rockwell C-33) was obtained on blades solution treated at 1950° or 2100° F (groups 2, 3, and 5). The blades having best engine life (group 1, solution treated for 1 hr at 2150° F) had a hardness of Rockwell C-31. The blades of group 4 that were forged at 1950° F but given the same heat treatment as group 1 had an intermediate hardness of Rockwell C-29.

All groups lost from 5 to 12 Rockwell C- units of hardness during engine operation with the exception of group 6 (initially the softest), which increased in hardness by 5 Rockwell C- units.

BLADE-FAILURE MECHANISM

In addition to centrifugal stress, factors such as vibratory stresses, thermal shock, and corrosion may influence blade failure. The usual method of determining which of these factors is most important in causing blade failure is by examination of the characteristics of the fracture surface. Often, however, appearance alone does not reveal the primary cause of failure. For example, in elevated-temperature tensile fatigue tests (ref. 4), it was found that even though vibratory stresses superimposed on a mean load reduced the life of the material, fatigue characteristics were not always observed on the fractured surfaces. Additional information is needed, therefore, if the failure mechanism is to be defined with some degree of certainty.

In addition to the appearance of fractured surfaces, the following factors were taken into consideration:

(1) A comparison of the life of the blades in the engine with the predicted life based on stress-rupture considerations only (fig. 1(b)). Factors other than stress-rupture (e.g., vibratory stress and thermal shock) generally would tend to reduce the life below that predicted.

(2) A comparison of the location of actual blade fracture with the location predicted for stress-rupture fracture. The predicted location for stress-rupture fracture was defined in two ways: (a) by a consideration of the centrifugal-stress and temperature distribution along the blade airfoil (fig. 1), and (b) by a determination of the zone along the airfoil where maximum creep occurred during operation of the engine. Fractures occurring some distance from the point or zone predicted for stress-rupture failure would again indicate that factors other than stress-rupture contributed to the failure mechanism.

The minimums of the curves of figure 1(b) define the best possible lives that could be expected from the different groups of blades and also locate a point where fracture by stress rupture should occur. This point is about $2\frac{1}{8}$ inches from the base of the airfoil. The curves do not express the true scatter of the data but represent the average data. Thus the minimums could perhaps more correctly be represented by a scatter band or zone. The small sampling of data does not, however, seem to warrant the drawing of such a zone.

A more direct method of determining a zone of expected stress-rupture failures is to locate the region in the blades that exhibits maximum creep during operation of the engine. The Inconel 550 blades exhibited so little elongation that creep measurements could not be used to define the "critical zone." However, the S-816 blades used as a standard for comparison may be used for this purpose since they

exhibited considerable elongation during operation. It may be seen in figure 5, that the elongation of the S-816 in the zone $1\frac{1}{2}$ to $2\frac{1}{2}$ inches above the blade root was approximately twice that occurring in the gage lengths either above or below this zone. It should be noted that the critical point indicated on figure 1(b) occurs near the exact center of this zone.

The majority of failures (74 percent) occurred above the "critical zone" (fig. 13) in positions of low centrifugal stress, thus indicating that factors in addition to stress rupture contributed to the failure. It is interesting that all except two of the blades that failed outside the critical zone exhibited fatigue characteristics at the fracture edges and all the blades that failed in the critical zone showed stress-rupture characteristics.

A further indication that fatigue is contributing to the failure mechanism will be evident from the following discussion. In figure 12, the blade failure times are replotted at the stress levels that obtain at the location of the failures. (These levels may be obtained from fig. 1(a).) The stress-rupture curves shown in figure 12 were obtained from the stress-rupture data specimens cut from blade airfoils. Based on any reasonable extrapolation of the stress-rupture curves, the blade lives have been reduced by 70 to 90 percent of that predicted from stress-rupture consideration alone.

Preliminary results from a study of the effects of vibratory stresses in a tensile-fatigue test on Inconel 550 are given in table VI. These data were obtained by superimposing a vibratory load of $\pm 10,700$ psi (90 percent of the mean load) on a mean load of 11,900 psi at a test temperature of 1490° F. The specimens selected were obtained from the blades of this investigation and were identical to the stress-rupture specimens shown in figure 3.

The data indicate that as much as 80 percent of the stress-rupture life can be lost when a vibratory load is applied to test specimens of this alloy. This indicates that vibratory stress is the predominant contributing factor to the failure mechanism other than centrifugal stress.

The degree that vibratory stresses reduced the life at the point where most fractures occurred (3 in. from the base) may be only of academic interest, however. On the basis of stress rupture alone, the blades would have failed lower in the airfoil, in the critical zone, long before the times predicted for the 3-inch location discussed in the preceding paragraph. For example, the best group of blades (group 1) that had an average life in the engine of about

760 hours would have failed by stress rupture at about 1000 hours in the critical zone. Thus, from a practical viewpoint, the reduction in actual life was only of the order of 25 percent.

DISCUSSION

Operating Life of Different Blade Groups

The blades that were forged, solution treated, and aged at high temperatures (group 1; forged at 2150° F, solution treated at 2150° F, and aged at 1600° and 1350° F) performed considerably better in the engine than the blades of all other groups, including the S-816 blades. Among specimens given the same heat treatments, a forging temperature of 2150° F proved superior to a forging temperature of 1950° F, as evidenced by the superior performance of the blades of group 1 relative to the blades of group 4. Among groups of blades forged at 2150° F, the group solution treated at 2150° F (group 1) was definitely superior to the group solution treated at 1950° F (group 3). Further evidence indicating superiority of high-temperature solution treatment may be obtained by comparing groups 4 to 6 with groups 2 and 3. Groups 4 to 6 solution treated at 2100° to 2150° F are superior to groups 2 and 3 solution treated at 1950° F, even though groups 2 and 3 were forged at a higher temperature. A comparison of group 2 with group 3 shows that, for equal solution-treating temperature, the two aging treatments appeared to yield equivalent engine performance.

The blades that performed best in this investigation (group 1) had the largest grain size and greatest range of grain size, and specimens cut from these blades exhibited the highest stress-rupture properties. Other than these differences, there appeared to be nothing that would distinguish this group of blades from all others. For example, there were no consistent trends in the hardnesses that could explain the performance of the various groups of blades, particularly of the best group. Furthermore, it was impossible to correlate engine performance of the different blade groups to microstructure, since, as has been noted, consistent differences in visible microstructure from blade to blade or group to group were not observed.

Elongation of Inconel 550 Blades

In past investigations, elongations of blades during engine operation were less than elongations of specimens cut from blade airfoils in stress-rupture tests when both tests were conducted under similar conditions of stress and temperature. Examples may be noted in the work

3562

CL-2 back

of reference 5, in which most of the S-816 stress-rupture specimens had elongations of the order of 21 percent, whereas elongation of the blades ranged from 4 to 12 percent.

The reason for the differences in elongation between blade airfoils and stress-rupture bars may be attributed to many factors. For example, it has been reported that total elongation of a test specimen is decreased when a superimposed fatigue load is placed upon it (refs. 4 and 6), and it may be assumed that the vibrations present in a blade during operation decrease the total elongation.

In this investigation, the Inconel 550 stress-rupture specimens showed elongations of 3 percent or more (table II), but blade airfoils elongated less than 0.3 percent in engine operation. In the past, materials exhibiting such low elongations have been considered too brittle for use. However, the performance of Inconel 550 blades was superior to that of S-816 blades, which had greater ductility. Also, the Inconel 550 blades did not fail from impact of blade fragments, as do certain cast alloys or inherently brittle materials such as cermets.

Grain Size

The concept that large-grained structures are stronger than fine-grained structures at high temperatures has been partially verified in several engine tests of cast alloys of different grain sizes (refs. 7 and 8). For example, in engine tests, coarse-grained blades of Stellite 21 and of 73J were superior to fine-grained blades. However, to obtain the larger grain sizes, it was necessary to vary fabrication methods. On the other hand, there is evidence (refs. 9 and 10) that high-temperature fatigue properties are reduced with an increase in grain size.

In this investigation the differences in grain size between the various groups (fig. 8) were so small as to preclude a detailed correlation of engine performance with grain size. These small differences in grain size were not expected as results of the fabrication procedures employed. For example, based on preliminary tests, the low forging and high solution-treating temperatures used for group 6 were expected to produce germinated ("elephant") grains. However, blades of this group did not exhibit evidence of this type of germination, but had grain sizes essentially similar to those of the other groups.

This lack of grain-size response to the different combinations of fabrication procedure and heat treatment may be due to the fact that the amount of cold-work introduced by forging was not of the critical amount necessary to promote growth of huge grains.

Significance of Hardness Measurements

As was pointed out, blades solution treated at 1950° or 2100° F (groups 2, 3, and 5) had higher hardnesses than those solution treated at 2150° F. Hardness was not influenced by increasing the forging temperature from 1950° to 2150° F. Thus, the hardnesses of groups 2 and 3 (forged at 2150° F) and group 5 (forged at 1950° F) were the same, Rockwell C-33. The lowest hardnesses were associated with the highest solution temperatures. If the aging treatments are assumed to be essentially equivalent, this trend in hardness may be explained by the fact that, at high solution temperatures, the hardening elements may be dispersed in the matrix in such a manner that longer aging times are required to nucleate precipitants. On this basis, the lowest hardness would be expected for blades of group 6 (solution treated 4 hr at 2150° F), and this proved to be the case.

In regard to the influence of operating time, group 6 blades increased in hardness, whereas blades of the other five groups decreased in hardness with increase in operating time. This increase in hardness of the originally softest group emphasizes the fact that the higher-temperature solution treatment (presumably obtained in this group) did not permit full hardening of the alloy at the aging temperature and aging time used.

SUMMARY OF RESULTS

This investigation was conducted to determine the influence of forging temperature and heat treatments upon the turbojet-engine performance of Inconel 550. The following results were obtained:

1. The best engine performance was associated with a forging and solution temperature of 2150° F. Reducing either the forging or solution temperature to 1950° F reduced the blade life. However, it appeared less damaging to reduce the forging temperature to 1950° F, if the solution temperature was above 2100° F, than to reduce the solution temperature to 1950° F after forging at 2150° F.
2. Blade life of the best group ranged from 450 to 857 hours, whereas the S-816 stock blades ran from 204 to 599 hours.
3. Fatigue characteristics were associated with almost all Inconel 550 and S-816 blade failures.
4. Blade performance could not be correlated with grain size. However, best performance was obtained from the group of blades having the

largest grains and greatest scatter in grain size, even though fatigue was associated with the failures. Both fine and coarse grains were found in most blades, but no "elephant" grains were found.

5. Engine performance could not be correlated with the microstructure of the alloy, since microstructural differences from blade to blade and within a single blade were greater than the differences among the various groups of blades. Microstructures after engine operation seemed generally the same as before operation. The only differences noted were more rapid response to etchants after engine operation and the appearance of depletion zones in the outer surfaces of the operated blades.

6. The highest hardness of heat-treated blades was associated with a solution-treating temperature of 1950° and 2100° F. Increasing the degree of solution had a tendency to reduce the heat-treated hardness (the hardness after aging) but permitted an increase in hardness to occur during engine operation.

Lewis Flight Propulsion Laboratory
National Advisory Committee for Aeronautics
Cleveland, Ohio, June 15, 1955

REFERENCES

1. Anon.: Inconel "X" - A High Strength, High Temperature Alloy. Data and Information. Rev. ed., Dev. and Res. Div., The International Nickel Co., Inc., Jan. 1949.
2. Anon.: INCO Current Data Report No. 1 - Creep Rupture Test Data - Inconel "X" Type 550. Huntington Works Lab., The International Nickel Co., Inc., Huntington (W. Va.).
3. Kemp, Richard H., and Morgan, William C.: Analytical Investigation of Distribution of Centrifugal Stresses and Their Relation to Limiting Operating Temperatures in Gas-Turbine Blades. NACA RM E7L05, 1948.
4. Ferguson, Robert R.: Effect of Magnitude of Vibratory Load Superimposed on Mean Tensile Load on Mechanism of and Time to Fracture of Specimens and Correlation to Engine Blade. NACA RM E52L17, 1952.
5. Garrett, F. B., Gyorgak, C. A., and Weeton, J. W.: Behavior of Forged S-816 Turbine Blades in Steady-State Operation of J33-9 Turbojet Engine with Stress-Rupture and Metallographic Evaluations. NACA RM E52L17, 1953.

6. Lazan, B. J., and Westberg, E.: Properties of Temperature-Resistant Materials under Tensile and Compressive Fatigue Tests. WADC Tech. Rep. 52-227, Wright Air Dev. Center, Wright-Patterson Air Force Base, Nov. 1952. (Contract AF 33(038) 18903, RDO No. 614-16.)
7. Hoffman, C. A., and Gyorgak, C. A.: Investigation of Effects of Grain Size upon Engine Life of Cast AMS 5385 Gas Turbine Blades. NACA RM E53D06, 1953.
8. Johnston, James R., Gyorgak, Charles A., and Weeton, John W.: Engine Performance of Alloy 73J Turbine Blades Cast to Predetermined Grain Sizes. NACA RM E54E05, 1954.
9. Toolin, P. R.: The Effect of Grain Size Upon the Fatigue Properties at 80, 1200, and 1600F of the "Precision-Cast" Co-Cr-Ni-W Alloy X-40. Sci. Paper 1663, Westinghouse Res. Labs., May 13, 1952.
10. Toolin, P. R., and Mochel, N. L.: High-Temperature Fatigue Strengths of Several Gas Turbine Alloys. Proc. A.S.T.M., vol. 47, 1947, pp. 677-691; discussion, pp. 692-694.

TABLE I. - FORGING TEMPERATURES AND HEAT TREATMENTS
USED IN PRODUCING INCONEL 550 TURBINE BLADES

Group	Forging temperature, °F	Solution treatment		First aging treatment		Second aging treatment	
		Temperature, °F	Time, hr	Temperature, °F	Time, hr	Temperature, °F	Time, hr
1	2150	2150	1	1600	4	1350	4
2		1950	4	1550	24	1300	20
3		1950	4	1600	4	1350	4
^a 4	1950	2150	1	1600	4	1350	4
^a 5		2100	4	1550	24	1300	20
^b 6		2150	4	1550	24	1300	20

^aAMS heat treatment for Inconel X.

^bCombination of forging temperature and solution treatment known to produce germinated grains.

TABLE II. - STRESS-RUPTURE LIFE AT 1500° F OF INCONEL 550 BAR STOCK
AND SPECIMENS TAKEN FROM BLADES

Specimen	Stress, psi					
	30,000		25,000		20,000	
	Life, hr	Elongation/in. gage length, percent	Life, hr	Elongation/in. gage length, percent	Life, hr	Elongation/in. gage length, percent
Bar stock	130.5	6.6	^a 320.0		739.4	3.3
Group 1	3.0	1.6	343.0	3.1	629.8 659.5 806.7	3.1 9.4 (b)
2	29.6	0	221.5	3.1	406.1 522.3 524.6	3.1 3.1 6.2
3	66.1	0	137.0	3.1	265.6 570.5 574.5	1.6 18.8 3.1
4					686.9 791.6	0 3.1
5	68.2	0	108.3	3.1	463.8 469.5 642.7	3.1 0 3.1
6	156.4	6.2	392.7	1.6	263.7 557.6 ^c 622.6	31.2 1.6 3.1

^aValue obtained from fig. 13.

^bNot determined - fragment missing from gage length.

^cAt stress for total of 638.6 hr - 16 hr at room temperature.

TABLE III. - BLADE-FAILURE MECHANISMS AND POSITION OF FAILURE ORIGIN FOR VARIOUS OPERATING TIMES

[Results of engine operation of turbine blades.]

Order of failure	Time at rated speed, hr	Type of failure (a)	Location of failure origin above base platform, in.	Location of failure with respect to edges (b)	Order of failure	Time at rated speed, hr	Type of failure (a)	Location of failure origin above base platform, in.	Location of failure with respect to edges (b)
Group 1					Group 5				
1	450.8	F	3.25	LE	1	418.0	F	3.0	LE
2	691.5	F	3.06	LE	2	450.8	F	3.25	LE
3	813.0	D	3.06	LE	3	581.5	D	---	---
4	815.0	F	2.75	TE	4	642.5	SR	2.38	C
5	848.5	SR	2.19	0.83 in. from LE	5	647.5	SR	2.31	0.38 in. from TE
6	857.5	F	2.75	LE	6	648.8	F	3.09	LE
7	857.5	F	2.75	LE	7	660.0	SR	2.44	C
Group 2					Group 6				
1	186.0	F	3.19	TE	1	278.4	F	3.0	LE
2	277.6	F	3.03	TE	2	290.0	F	3.08	LE
3	290.0	SR	2.88	C	3	390.8	F	3.12	LE
4	290.5	F	3.25	LE	4	486.8	F	3.0	LE
5	384.8	D	---	---	5	648.8	F	3.08	LE
6	560.5	F	3.25	LE	6	669.5	F	3.0	LE
7	766.2	F	3.09	LE	7	747.1	SR	2.06	0.62 in. from LE
Group 3					3-816 (standard for comparison)				
1	235.6	F	2.94	LE	1	203.5	F	2.38	TE
2	271.8	SR + F	2.78	LE	2	271.8	F	3.03	LE
3	290.0	D	---	---	3	275.5	F	2.31	TE
4	291.9	F	2.97	LE	4	290.0	F	2.44	TE
5	360.8	SR + F	3.06	C	5	290.0	D	---	---
6	369.0	SR	2.56	0.25 in. from TE	6	290.3	F	2.88	LE
7	540.5	SR + F	3.03	LE	7	543.8	F	2.53	LE
Group 4					8	599.8	F	2.50	LE
1	290.0	F	3.0	LE					
2	396.6	F	3.09	LE					
3	514.8	D	---	---					
4	581.5	F	3.06	LE					
5	653.4	F	3.09	LE					
6	675.2	F	3.03	LE					
7	813.0	D	---	---					

*F, fatigue; SR, stress-rupture; D, damage; SR + F, stress-rupture followed by fatigue.

*LE, leading edge; TE, trailing edge; C, center section chordwise.

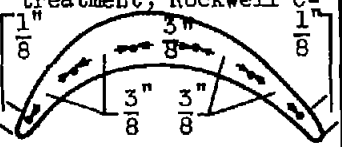
TABLE IV. - GRAIN SIZE OF VARIOUS BLADE GROUPS OF INCONEL 550

Group	Time to first failure, hr	Expected grain size (a)	Macro-grain size observed	A.S.T.M. grain size (b)
1	450	Medium to uniform	Medium to large	(9×1), 1, 7
2	186	Fine to medium	Fine to medium	(10×1), 1, 6
3	245	Fine to medium	Medium	(2 $\frac{1}{2}$ ×1), 2, 7
4	290	Coarse	Fine to medium	(32×1), 1, 7
5	278	Coarse-germinated	Fine to coarse	(1) , 5, 8
6	416	Coarse	Fine to coarse	(9×1), 1, 6

^a Expected grain size based on past investigations of nickel-base alloys.

^b Grain size based on A.S.T.M. grain-size numbers.
 First value - largest grains found, determined as a multiple of A.S.T.M. grain size number 1.
 Center value - size of most prevalent grains.
 Last value - size of smallest grains.

TABLE V. - ROCKWELL HARDNESS OF INCONEL 550 BLADES BEFORE AND AFTER OPERATING IN TURBOJET ENGINE

Alloy group	Hardness ^a of as-received blades after heat treatment, Rockwell C-						Average hardness ^a of as-heat-treated blades, Rockwell C-	Average ^b hardness ^a of first failed blades, Rockwell C-	Time to failure, hr	Average ^b hardness ^a of last failed blades, Rockwell C-	Time to failure, hr	Change in hardness from heat-treated to last failure
												
1	--	31	31	31	29	--	30.5	21	450.8	26	848.5	-4.5
2	--	34	33	33	31	--	33	24	186.0	21	788.2	-12
3	--	33	32.5	33.5	32.5	--	33	26	235.6	25	540.5	-8
4	--					--	^b 29	21	290.0	21.5	813	-7.5
5	--	33.8	33.8	33.8	30.5	--	33	25	418.0	25	660.0	-8
6	--	25.5	22	22.5	20	--	22.5	24.5	278.4	28	747.1	+5.5

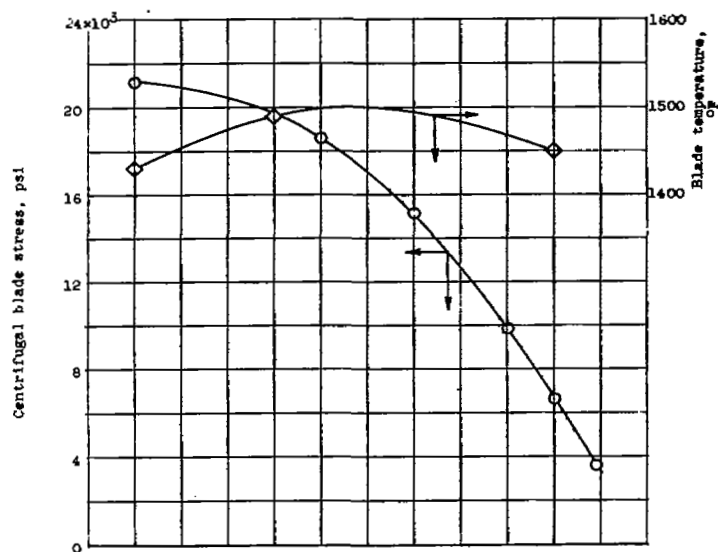
^aConverted from Rockwell-A readings.^bAverage of 10 readings over cross-sectional area.

TABLE VI. - TENSILE-FATIGUE DATA FOR INCONEL 550

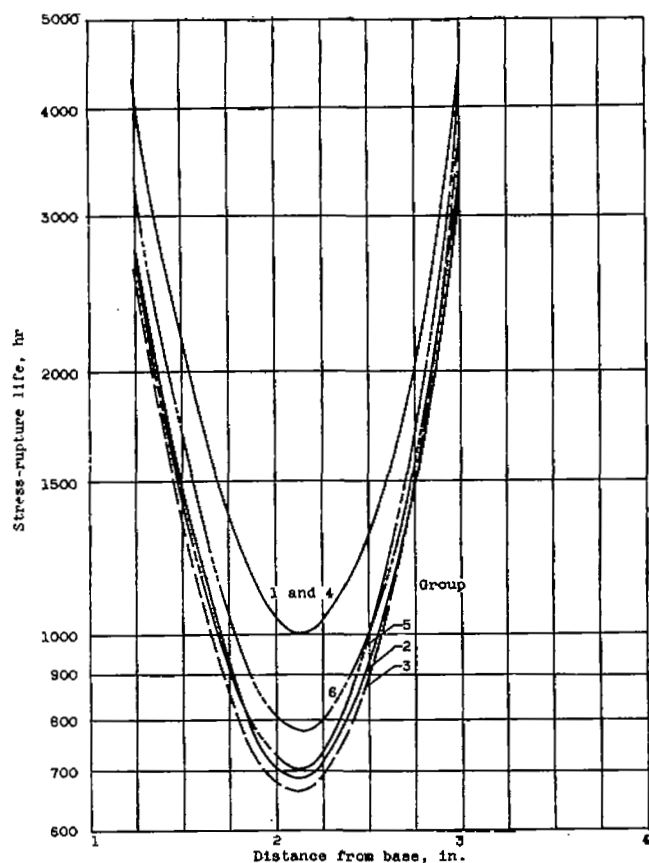
SPECIMENS AT 1490° F

[Load of $\pm 10,700$ psi superimposed on 11,900-psi mean load.]

Group	Time to failure, hr	Approximate stress- rupture life at 11,900 psi stress, hr	Approximate reduction in life, percent
1	2056.0	3100	34
2	551.7	2300	80
5	833.4	2500	67
6	961.3	2500	62

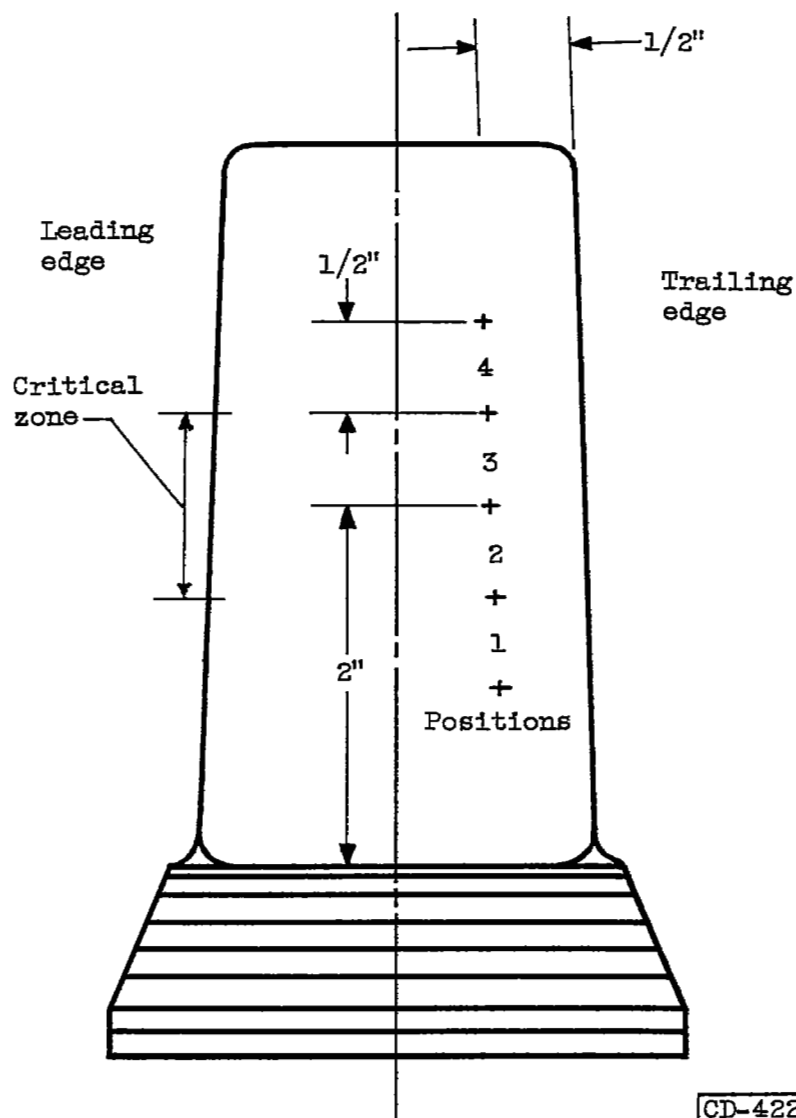


(a) Stress and temperature distribution.



(b) Stress-rupture life.

Figure 1. - Stress and temperature distribution in Inconel 550 turbine blade at rated speed and corresponding stress-rupture life of specimens cut from airfoils of group 1 blades.



CD-4222

Figure 2. - Location of scribe marks on convex side of turbine blade for use in measuring elongation.

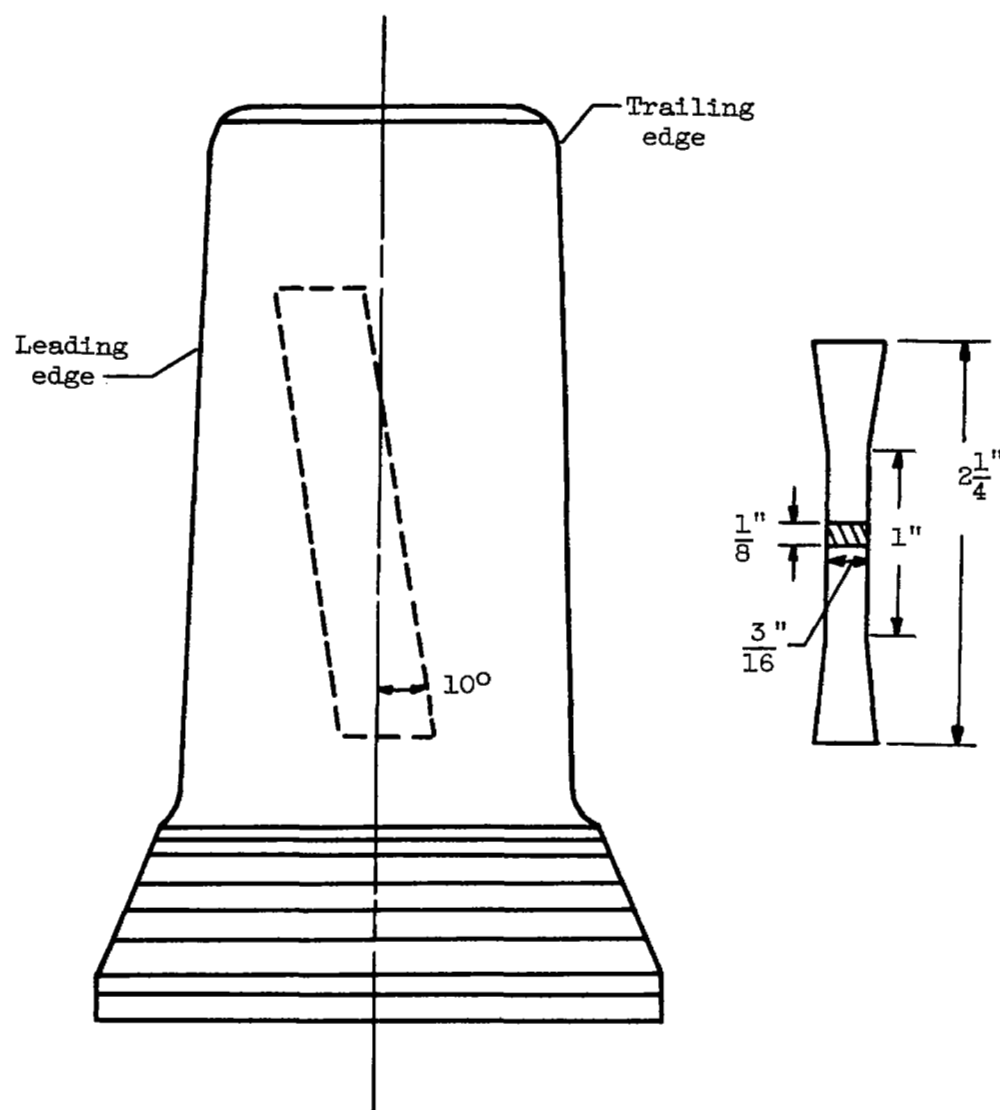


Figure 3. - Blade stress-rupture specimen and zone from which it was machined.

Group	Forging temperature, $^{\circ}\text{F}$	Solution treatment		First age treatment		Second age treatment	
		Temperature, $^{\circ}\text{F}$	Time, hr	Temperature, $^{\circ}\text{F}$	Time, hr	Temperature, $^{\circ}\text{F}$	Time, hr
1	2150	2150	1	1600	4	1350	4
2	2150	1850	4	1600	4	1350	4
3	2150	1850	4	1550	24	1300	20
4	1950	2150	1	1600	4	1350	4
5	1950	2100	4	1550	24	1300	20
6	1950	2150	4	1550	24	1300	20

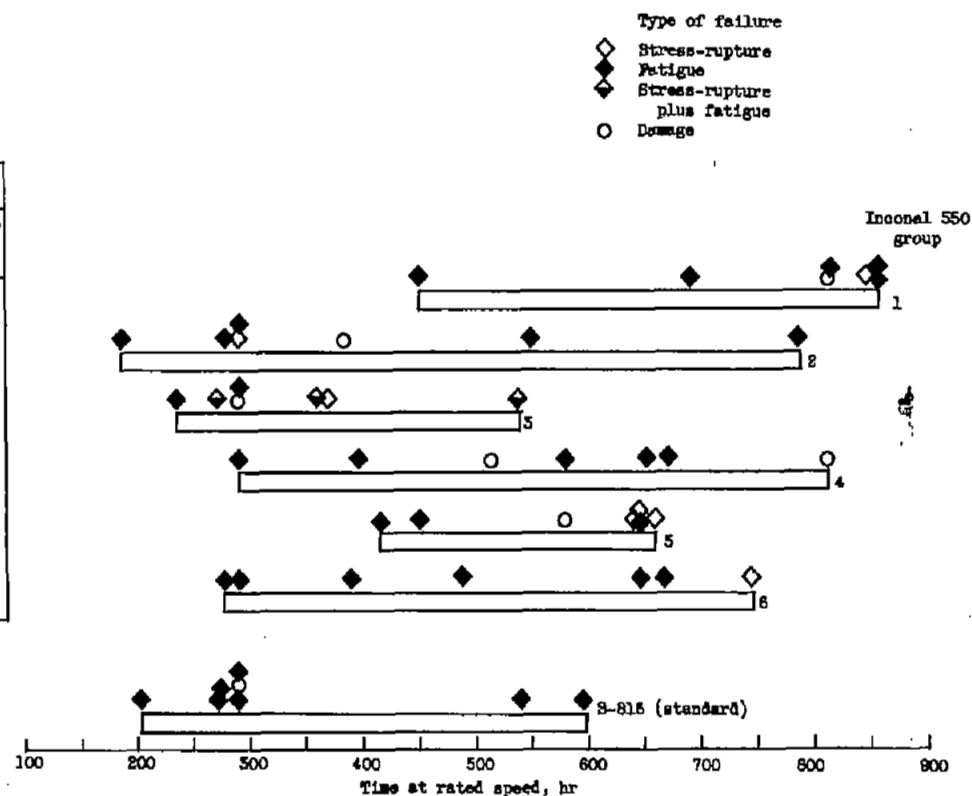


Figure 4. - Effect of forging temperature and heat treatment on blade life of Inconel 550 in turbojet engine.

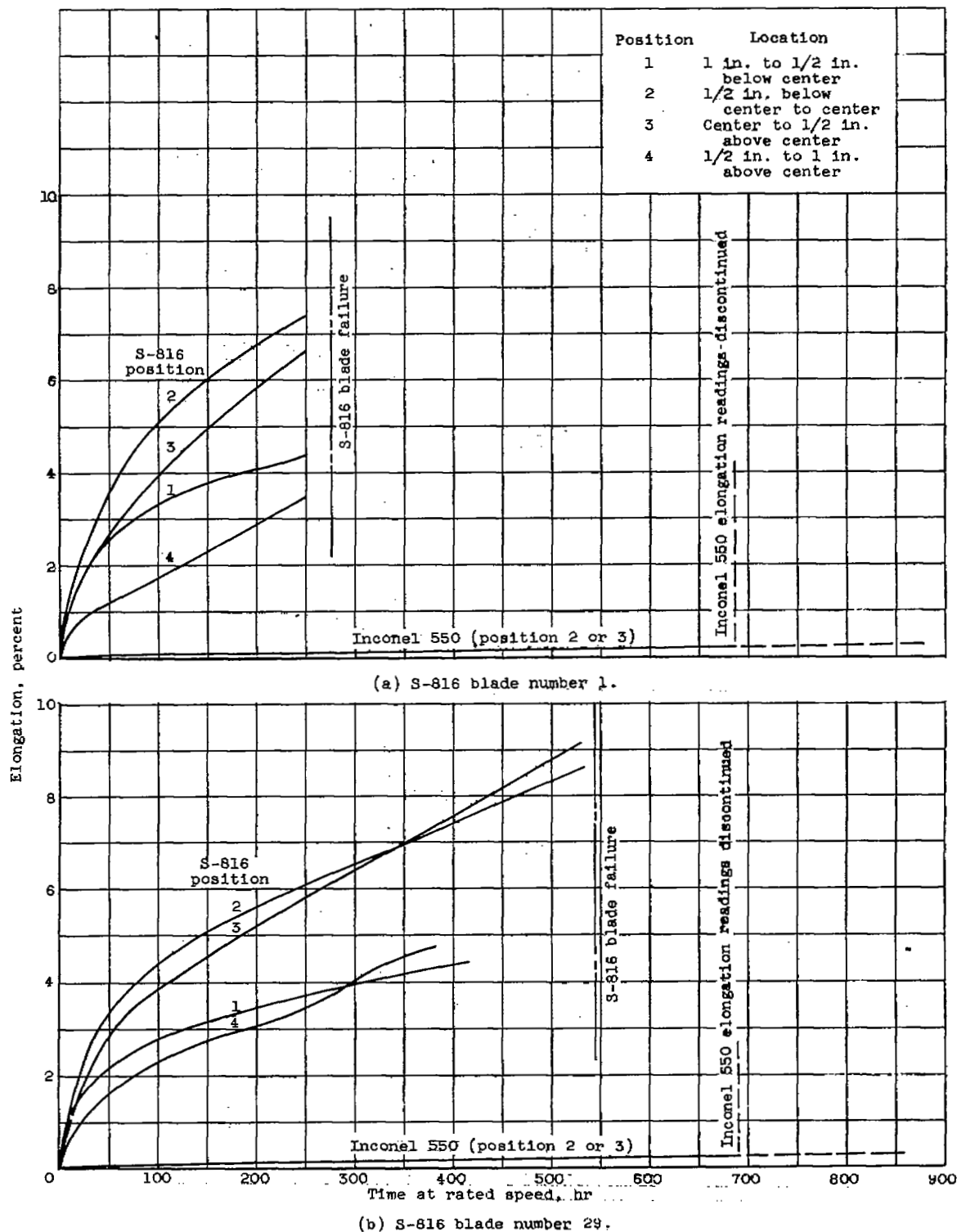
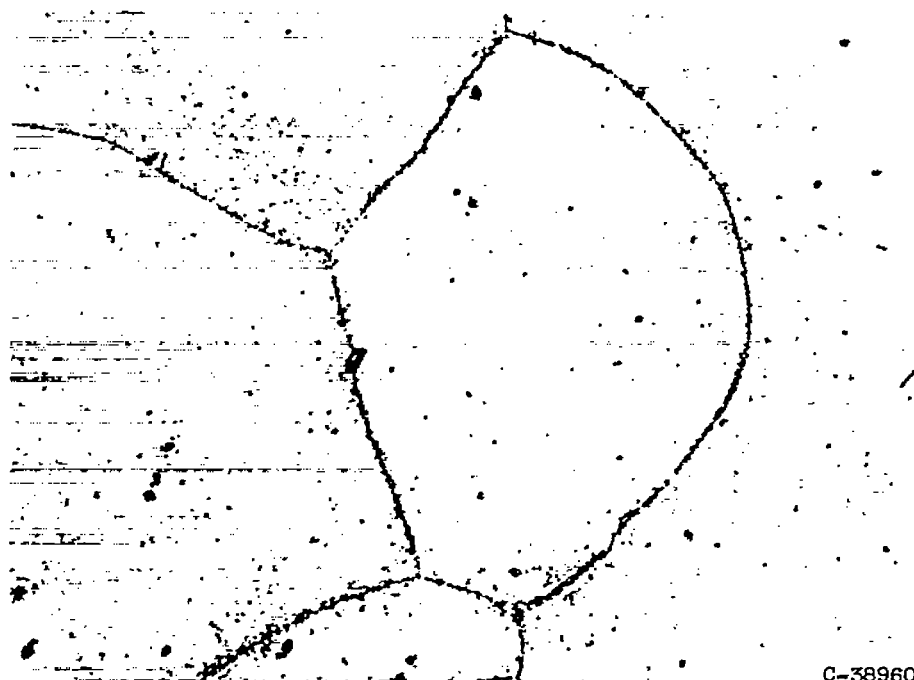


Figure 5. - Maximum elongation of Inconel 550 compared with elongation of S-816.

3562

CL-4 back



C-38960

Figure 6. - Typical microstructures of heat-treated Inconel 550. Etchant: 5 cc HF, 20 cc glycerine, 20 cc water; electrolytic. (Specimen taken from group 6 blade.) X750.



(a) Lamellar precipitate present in leading and trailing edges of blades that may have been cold-worked during forging. (Specimen taken from group 3 blade.)



(b) Precipitate in slip planes of grains in areas that may have been cold-worked during forging. (Specimen taken from group 1 blade.)

Figure 7. - Microstructures frequently observed in as-heat-treated Inconel 550 blades. Etchant: 5 cc HF, 20 cc glycerine, 20 cc water; electrolytic. X750.



(c) Depletion zone occurring along grain boundaries away from surface of blade. (Specimen taken from group 1 blade.)



C-38962

(d) Type of grain-boundary precipitate noted in localized areas of all groups of blades. (Specimen taken from group 1 blade.)

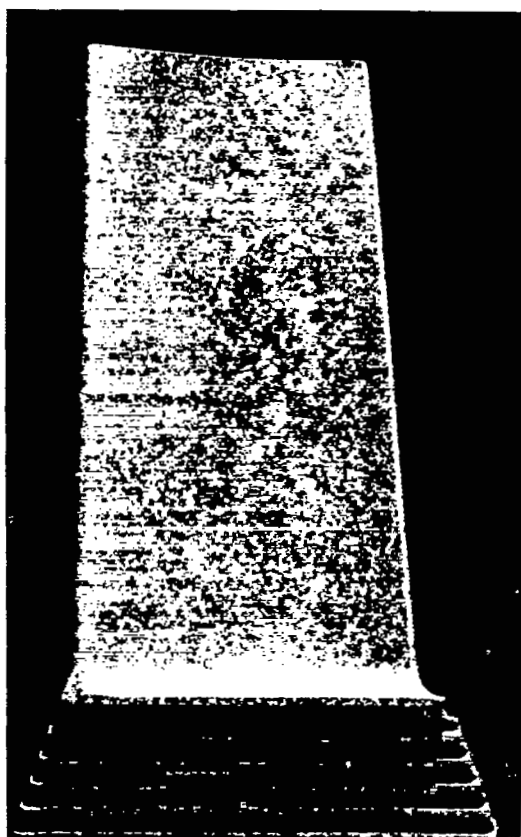
Figure 7. - Continued. Microstructures frequently observed in as-heat-treated Inconel 550 blades. Etchant: 5 cc HF, 20 cc glycerine, 20 cc water; electrolytic. X750.



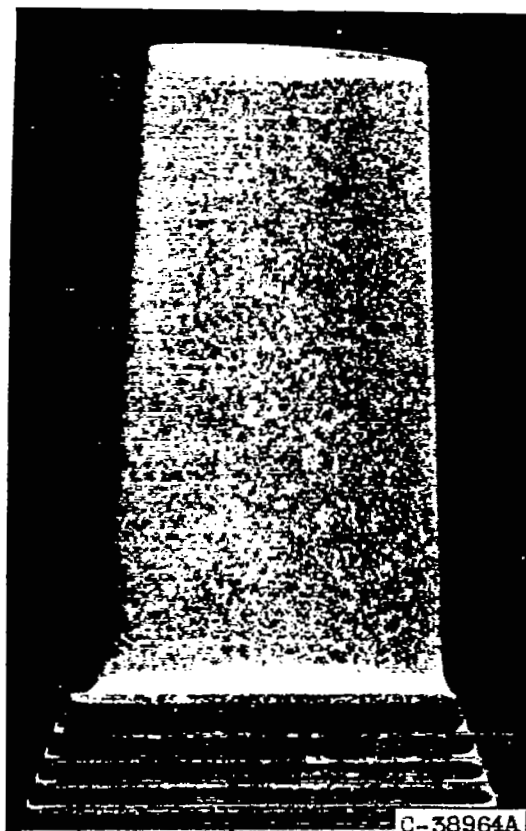
(e) Greatest quantity of grain-boundary precipitate noted.
(Specimen taken from group 1 blade.)

Figure 7. - Concluded. Microstructures frequently observed in as-heat-treated Inconel 550 blades. Etchant: 5 cc HF, 20 cc glycerine, 20 cc water; electrolytic. X750.

3562



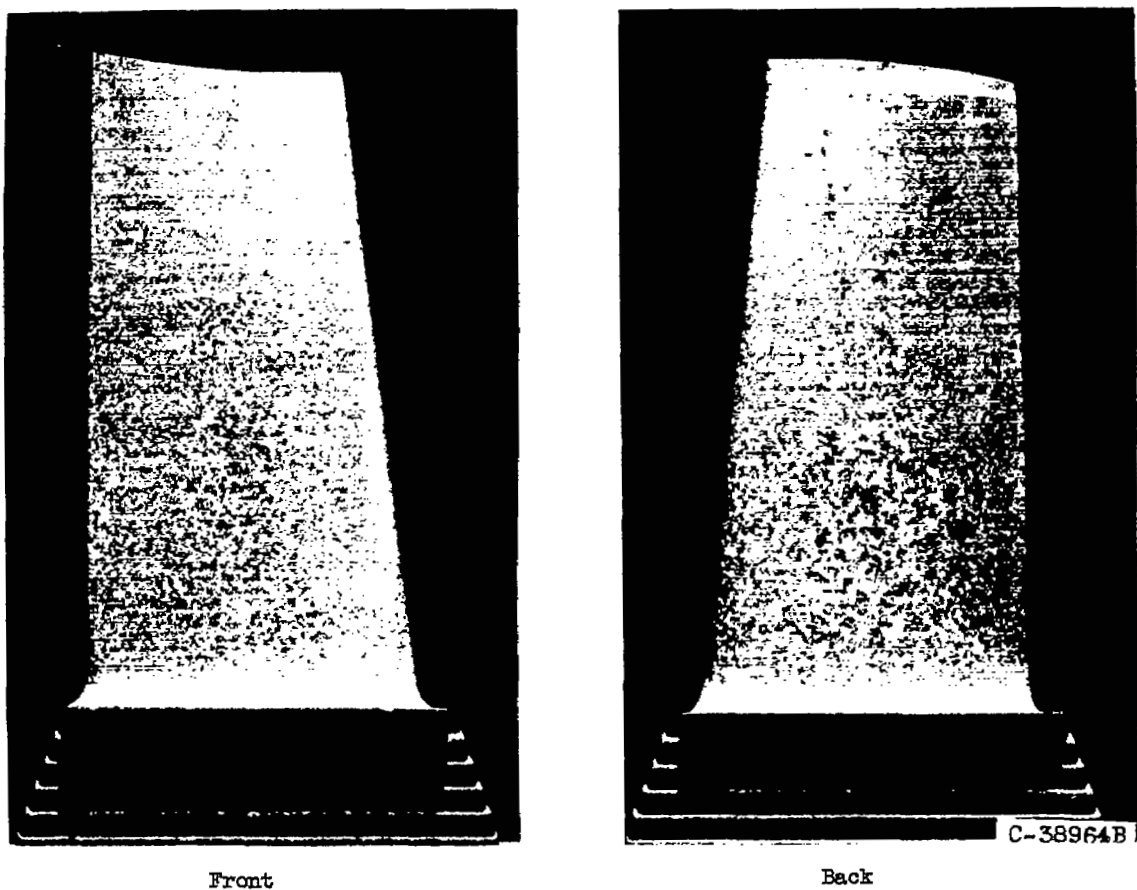
Front



Back

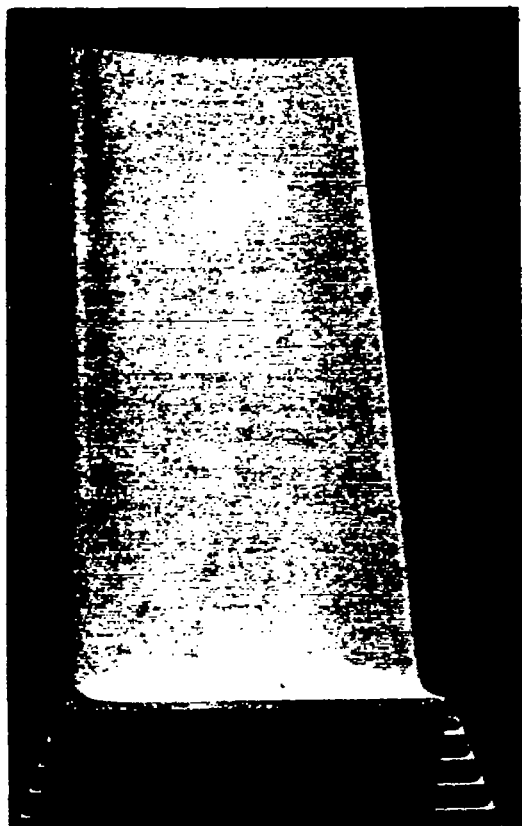
(a) Group 1 blade, largest grains noted.

Figure 8 - Macrograin size of Inconel 550 blades. Etchant: 80 parts concentrated HCl, 20 parts H_2O_2 ; immersion.

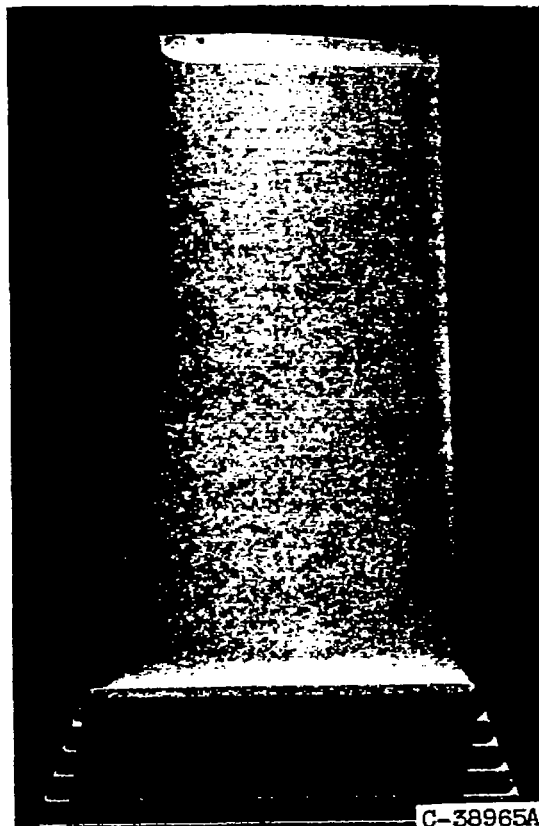


(b) Group 1 blade, smallest grains noted.

Figure 8. - Continued. Macrograin size of Inconel 550 blades. Etchant: 80 parts concentrated HCl, 20 parts H₂O₂; immersion.



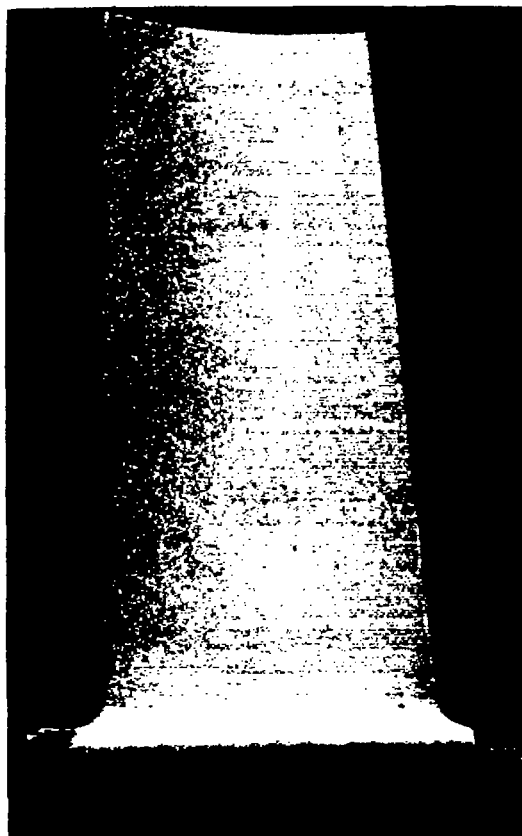
Front



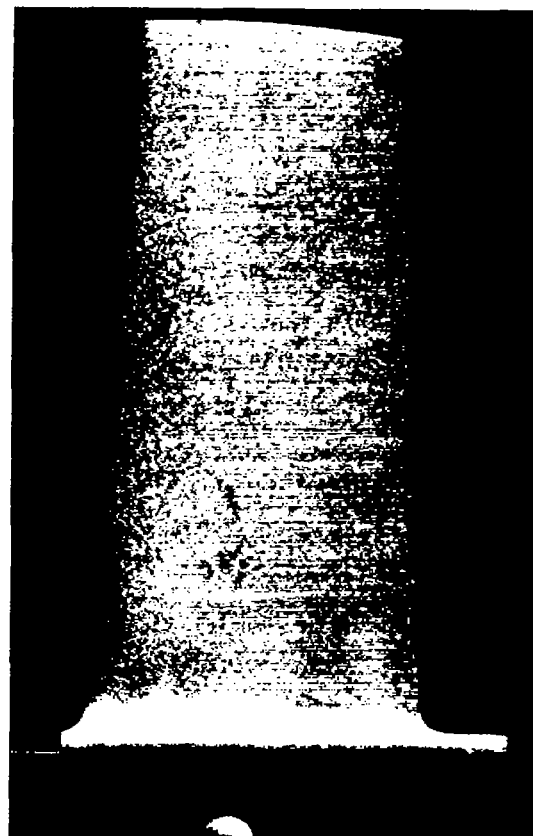
Back

(c) Group 2 blade, largest grains noted.

Figure 8. - Continued. Macrograin size of Inconel 550 blades. Etchant: 80 parts concentrated HCl, 20 parts H_2O_2 ; immersion.



Front

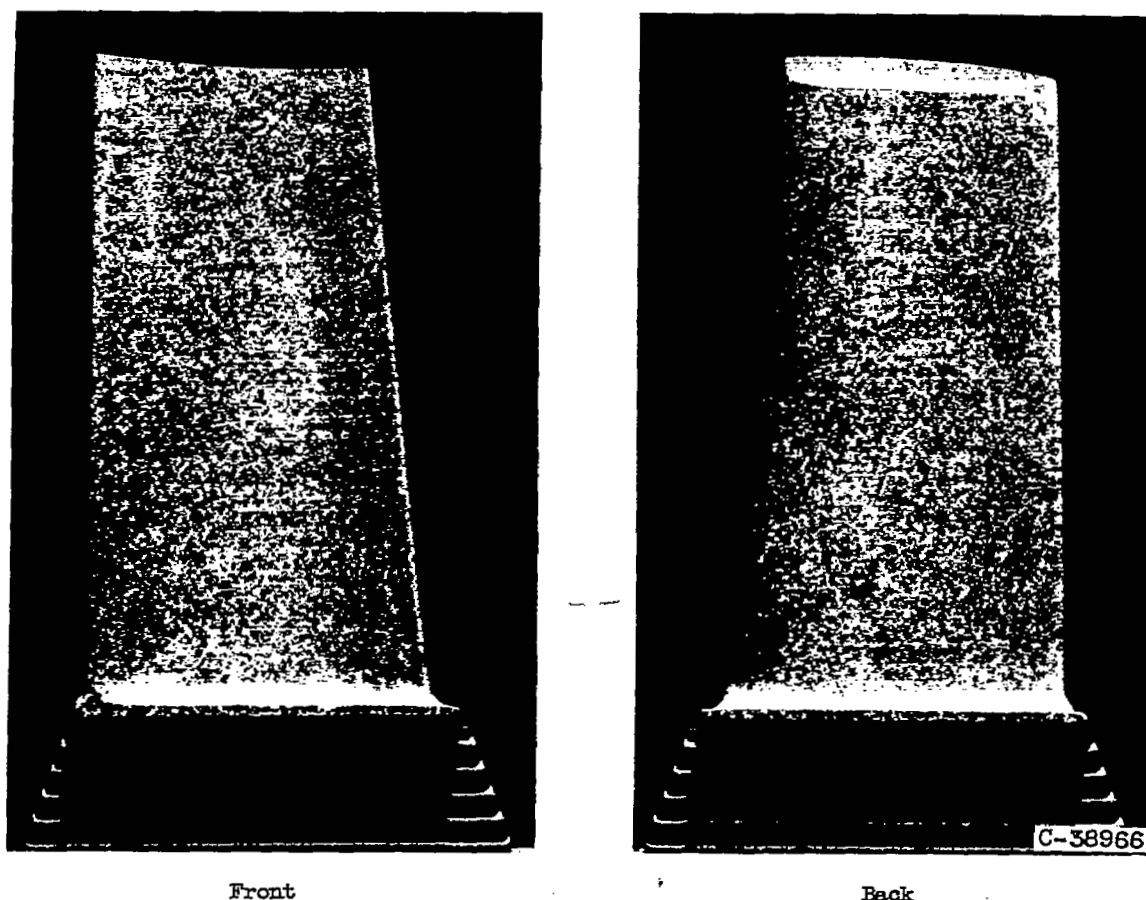


Back

C-38965B

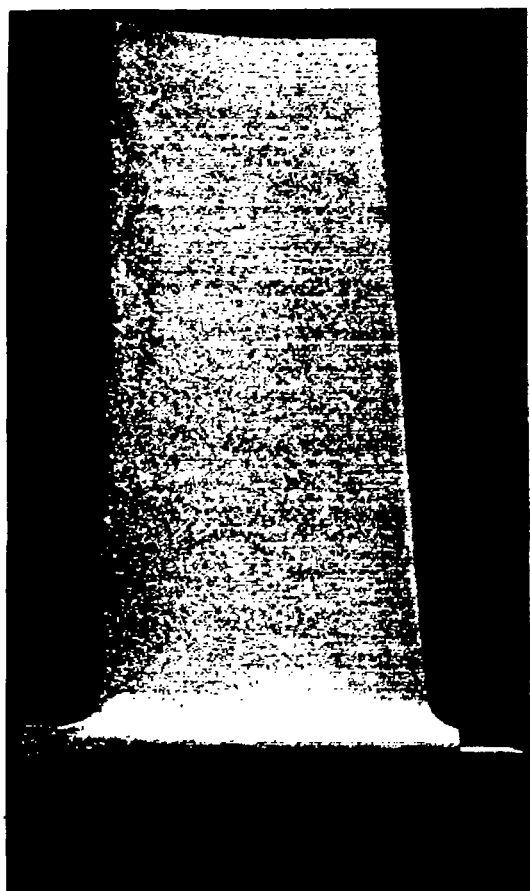
(d) Group 2 blade, smallest grains noted. (Blade did not meet dimensional tolerance.)

Figure 8. - Continued. Macrograin size of Inconel 550 blades. Etchant: 80 parts concentrated HCl, 20 parts H_2O_2 ; immersion.

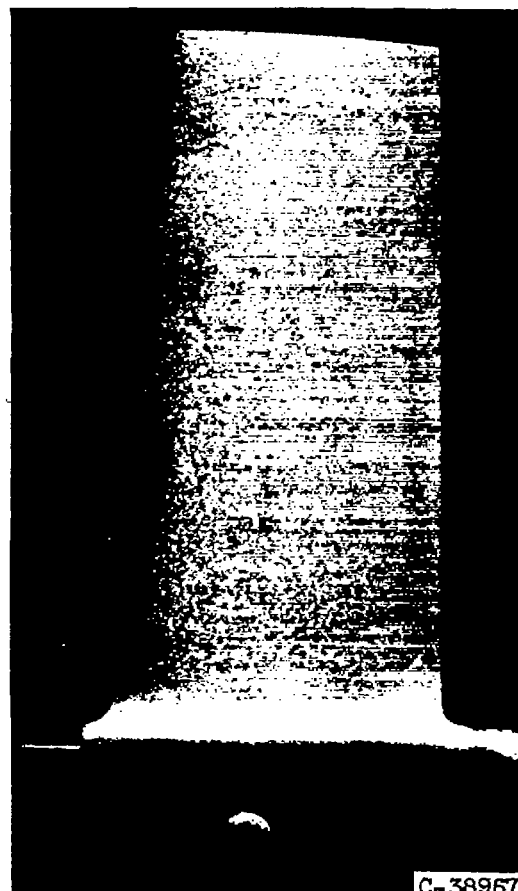


(e) Typical grain size of group 3 blades.

Figure 8. - Continued. Macrograin size of Inconel 550 blades. Etchant: 80 parts concentrated HCl, 20 parts H_2O_2 , immersion.



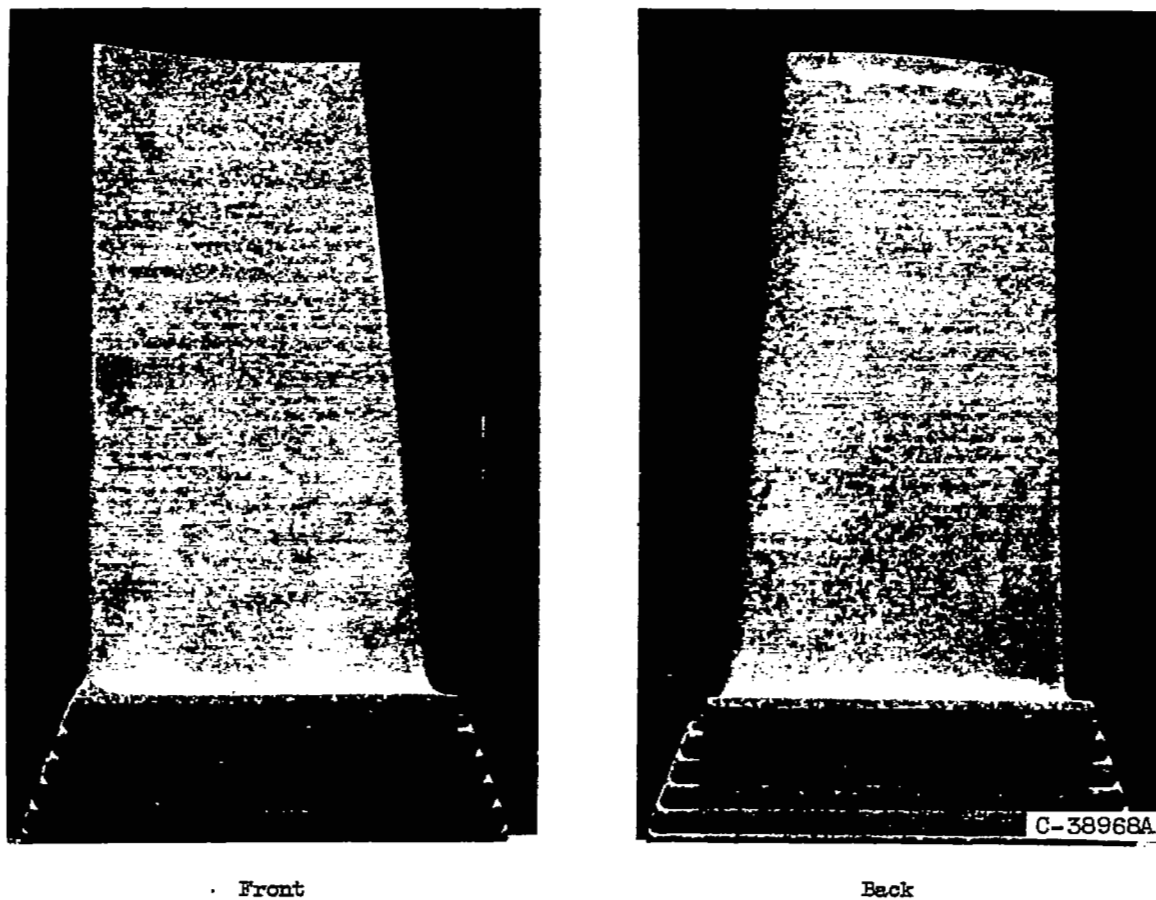
Front



Back

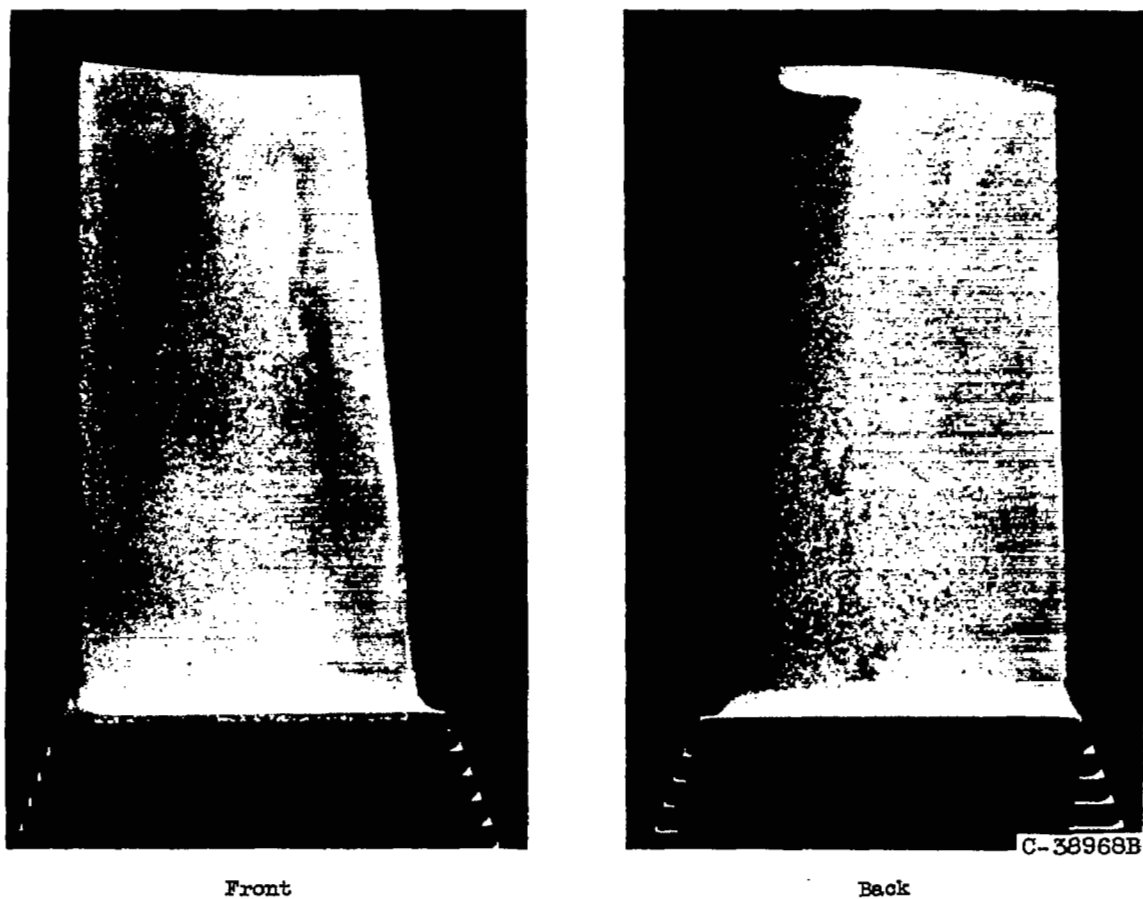
(f) Typical grain size of group 4 blades. (Blade did not meet dimensional tolerances.)

Figure 8. - Continued. Macrograin size of Inconel 550 blades. Etchant: 80 parts concentrated HCl, 20 parts H_2O_2 ; immersion.



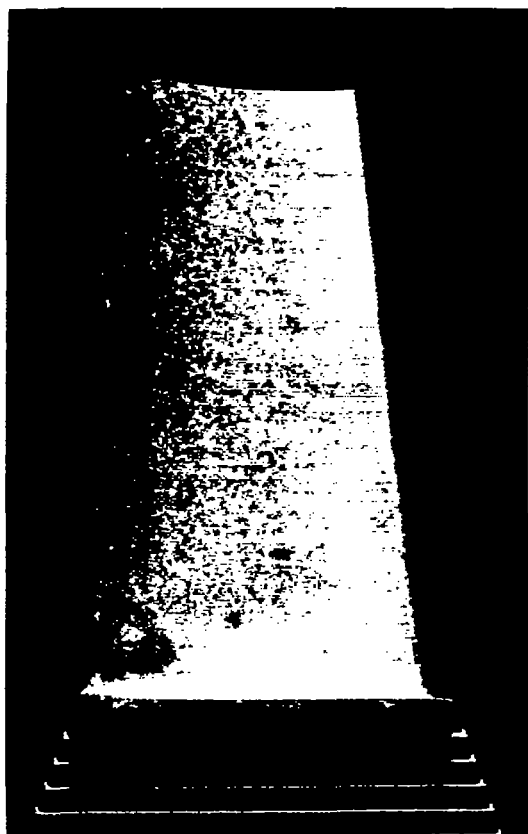
(g) Group 5 blade, largest grains noted.

Figure 8. - Continued. Macrograin size of Inconel 550 blades. Etchant: 80 parts concentrated HCl, 20 parts H₂O₂; immersion.

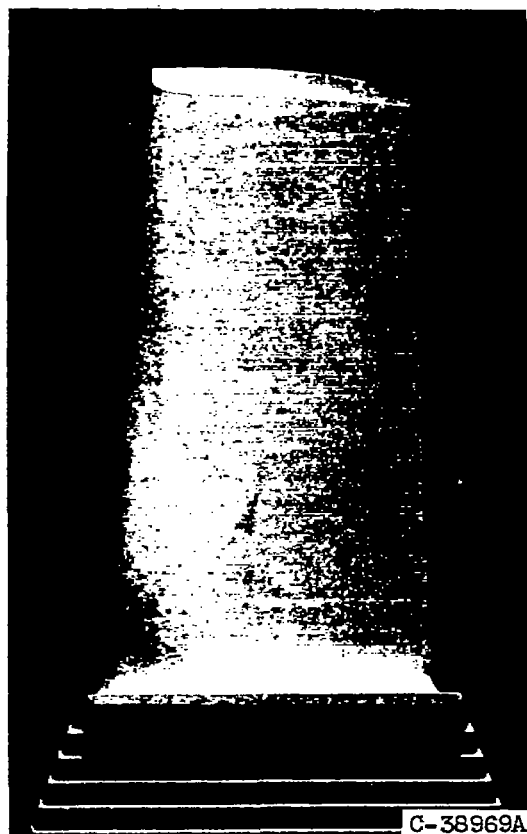


(h) Group 5 blade, smallest grains noted.

Figure 8. - Continued. Macrograin size of Inconel 550 blades. Etchant: 80 parts concentrated HCl, 20 parts H_2O_2 ; immersion.



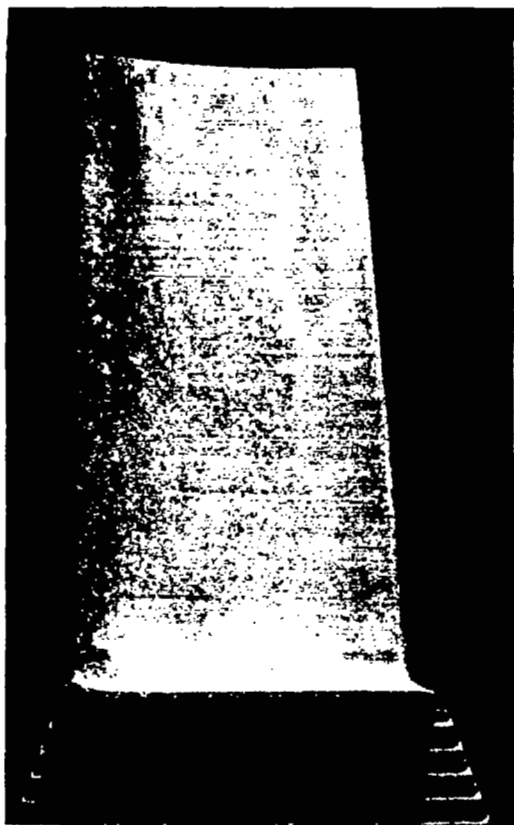
Front



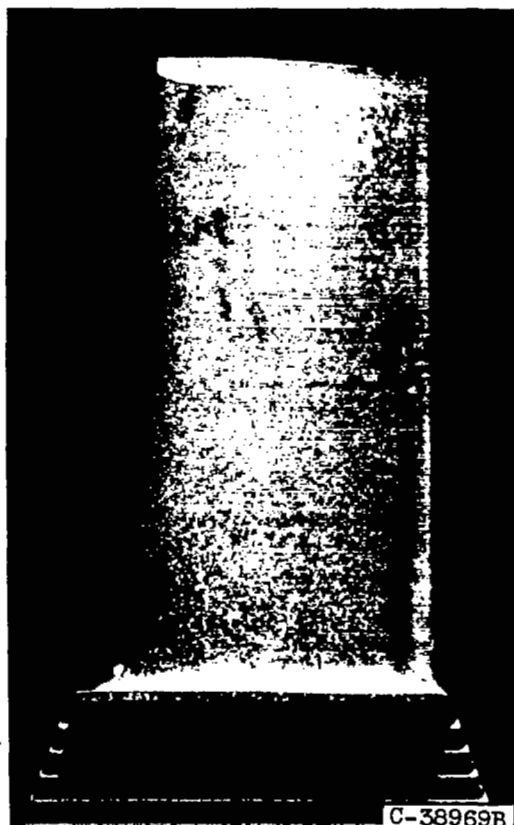
Back

(1) Group 6 blade, largest grains noted.

Figure 8. - Continued. Macrograin size of Inconel 550 blades. Etchant: 80 parts concentrated HCl, 20 parts H₂O₂; immersion.



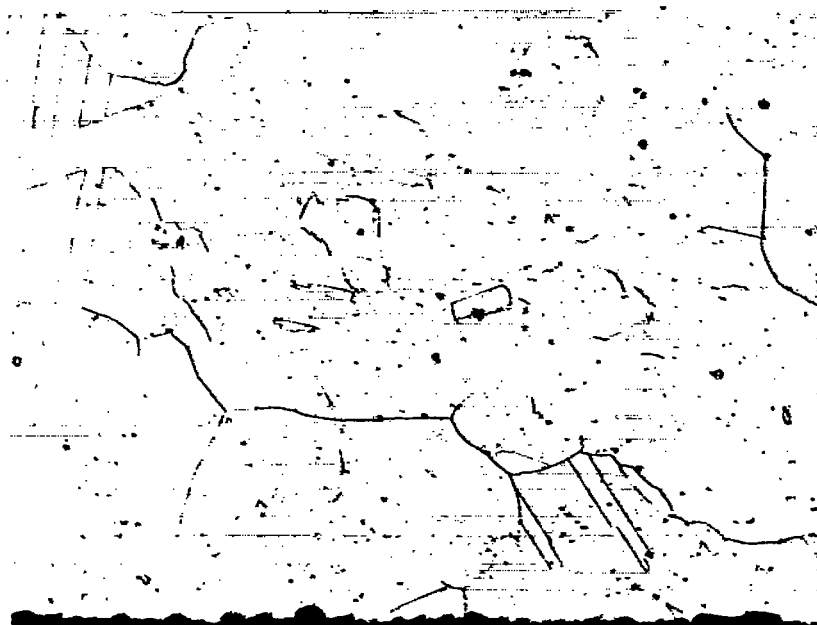
Front



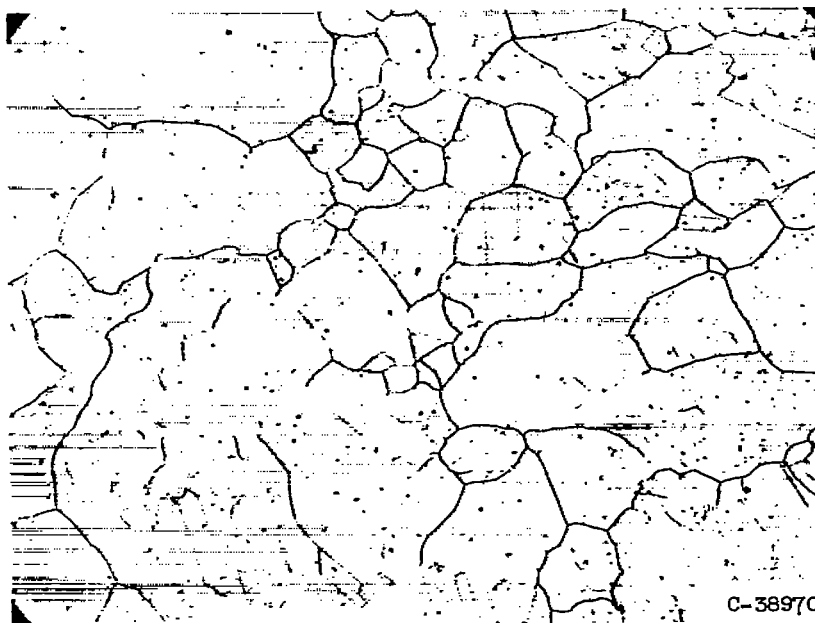
Back

(j) Group 6 blade, smallest grains noted.

Figure 8. - Concluded. Macrograin size of Inconel 550 blades. Etchant: 80 parts concentrated HCl, 20 parts H₂O₂; immersion.



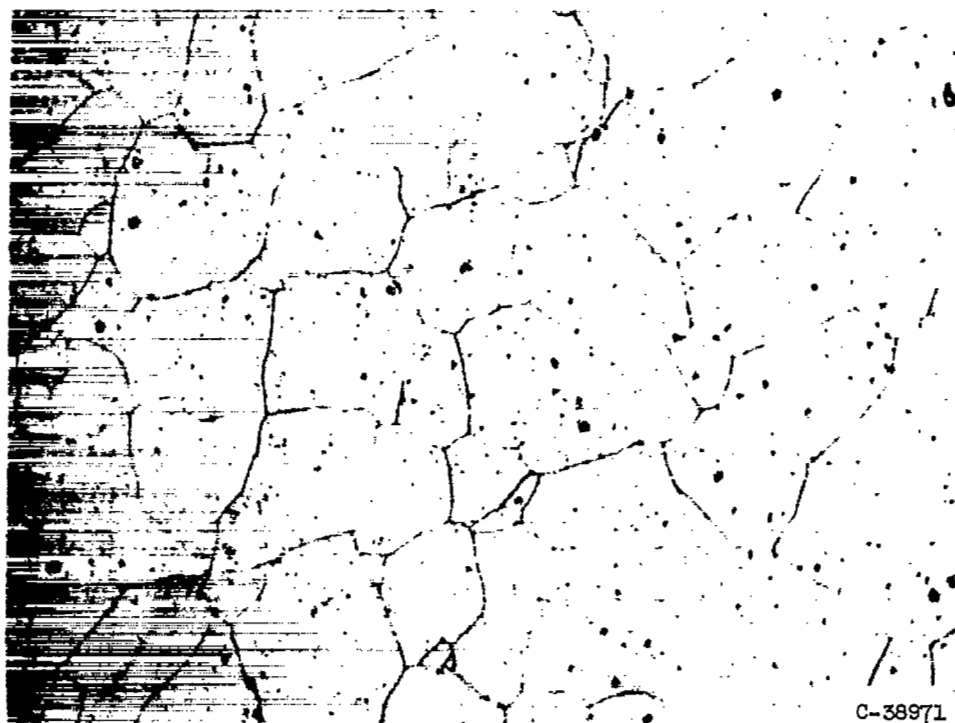
(a) Large grains occurring in trailing edge of group 1 blade. X100.



(b) Mixed grain size in cold-worked area of trailing edge of group 1 blade. X50.

C-38970

Figure 9. - Micrograin size of as-heat-treated Inconel 550 in cross-sectional specimens taken $2\frac{3}{16}$ inches above base platform of blades. Etchant: 5 cc HF, 20 cc glycerine, 20 cc water; electrolytic.

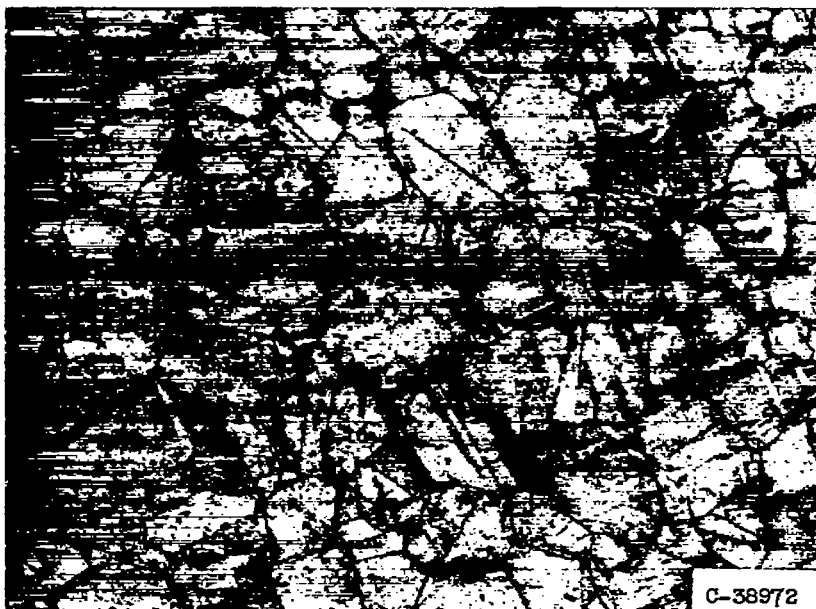


(c) Typical grain size in cross section of group 2 blade. X100.

Figure 9. - Continued. Micrograin size of as-heat-treated Inconel 550 in cross-sectional specimens taken $2\frac{3}{16}$ inches above base platform of blades. Etchant: 5 cc HF, 20 cc glycerine, 20 cc water; electrolytic.

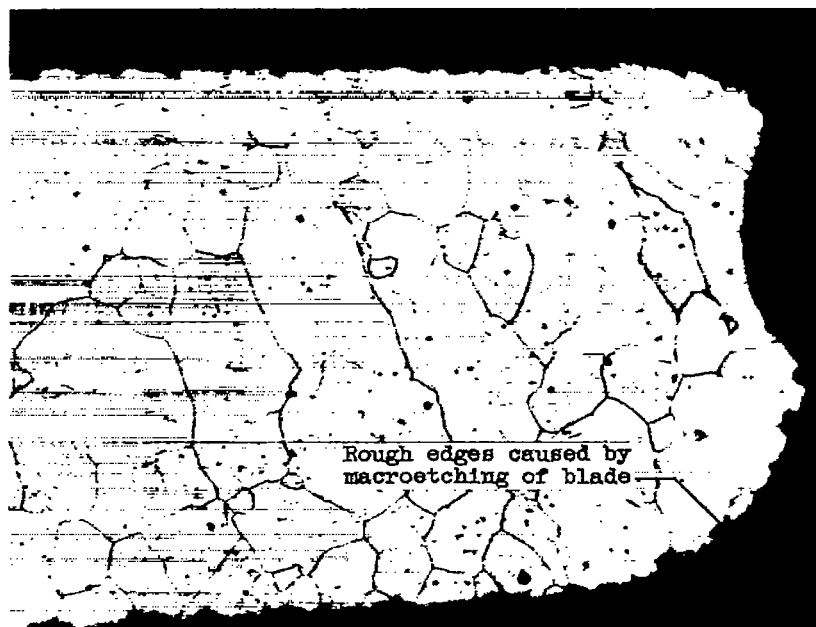


(d) Grain growth in surface cold-worked area of group 3 blade. X100.

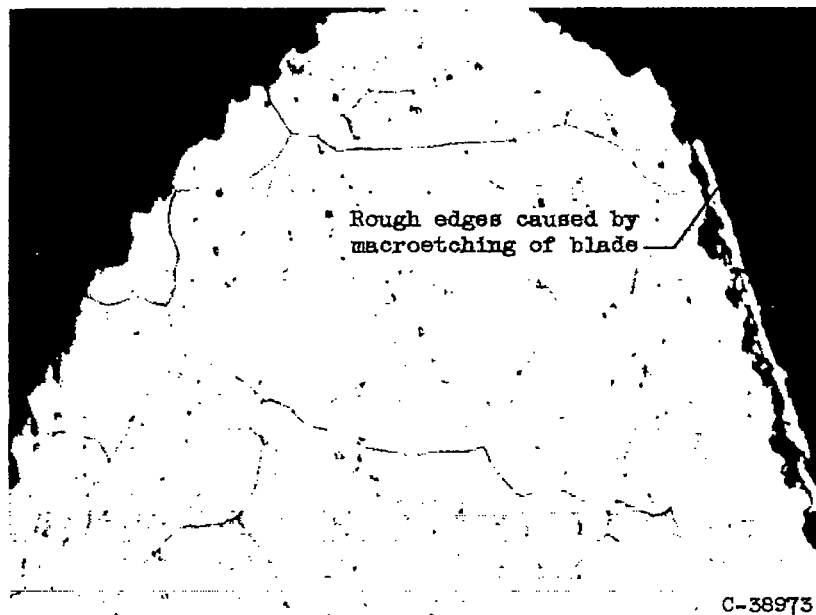


(e) Typical grain size of group 3 blade. X100.

Figure 9. - Continued. Micrograin size of as-heat-treated Inconel 550 in cross-sectional specimens taken $2\frac{3}{16}$ inches above base platform of blades. Etchant: 5 cc HF, 20 cc glycerine, 20 cc water; electrolytic.

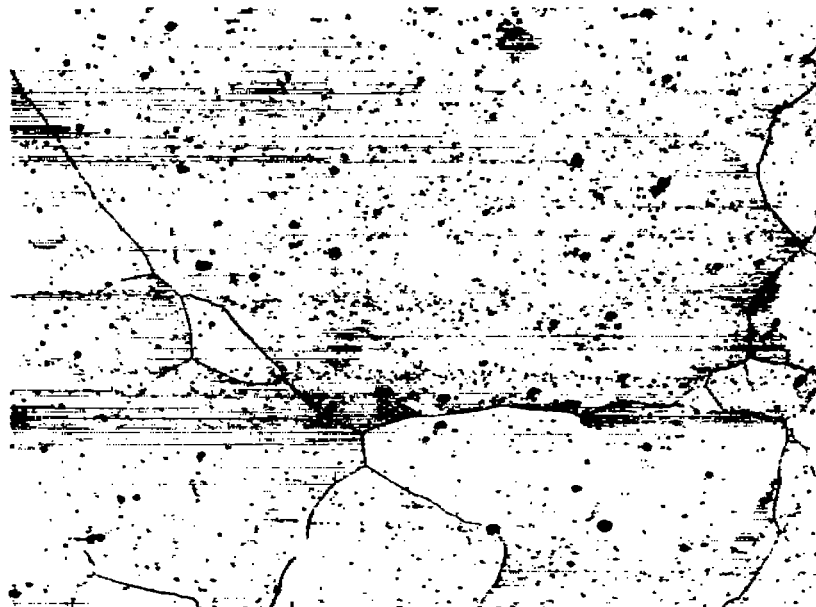


(f) Mixed grain sizes occurring in trailing edge of group 4—blade. X100.



(g) Large grains in leading edge of group 4 blade. X100.

Figure 9. - Continued. Micrograin size of as-heat-treated Inconel 550 in cross-sectional specimens taken $2\frac{3}{16}$ inches above base platform of blades. Etchant: 5 cc HF, 20 cc glycerine, 20 cc water; electrolytic.



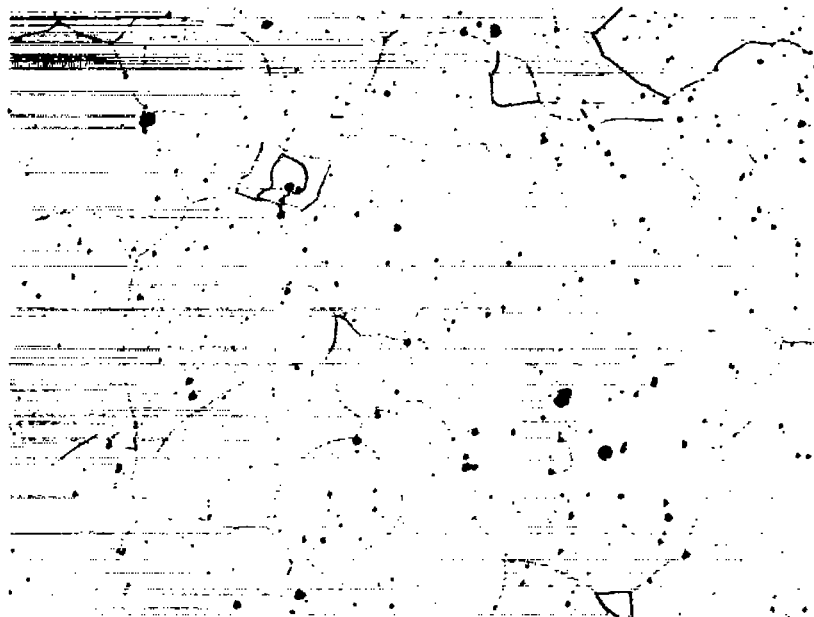
(h) Large grain in trailing edge of group 5 blade. X100.



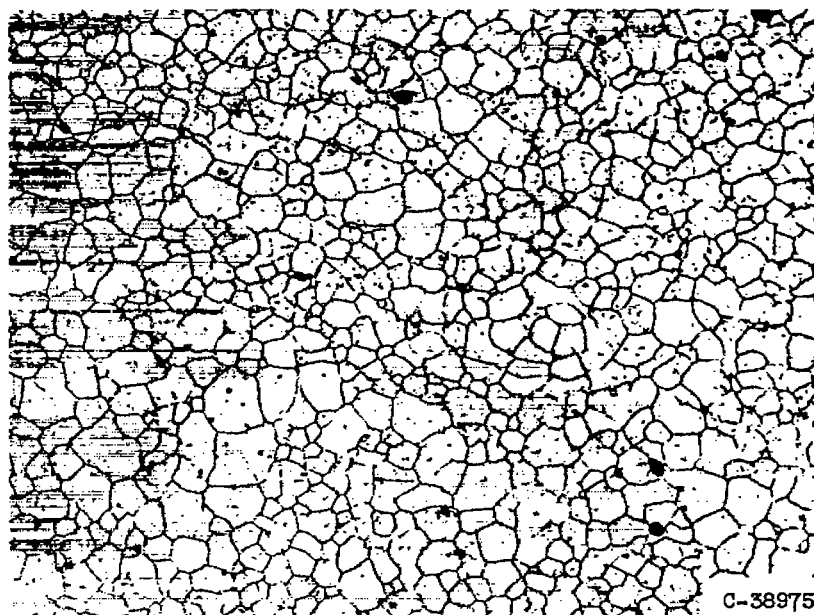
C-38974

(i) Average grain size of group 5 blade. X100.

Figure 9. - Continued. Micrograin size of as-heat-treated Inconel 550 in cross-sectional specimens taken $2 \frac{3}{16}$ inches above base platform of blades. Etchant: 5 cc HF, 20 cc glycerine, 20 cc water; electrolytic.

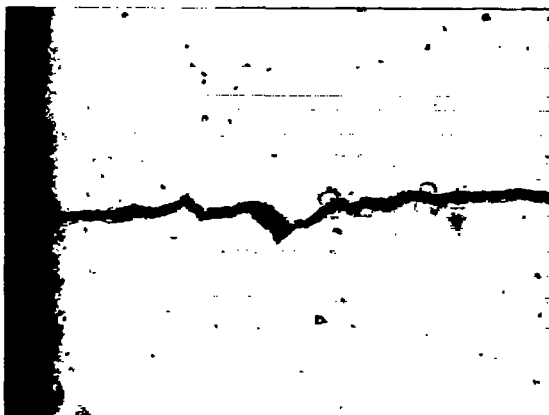


(j) Average grain size in group 6 blades. X100.



(k) Finest grain size occurring in Inconel 550 blades.
(Specimen taken from group 6 blade.) X100.

Figure 9. - Concluded. Micrograin size of as-heat-treated Inconel 550 in cross-sectional specimens taken $2\frac{3}{16}$ inches above base platform of blades. Etchant: 5 cc HF, 20 cc glycerine, 20 cc water; electrolytic.



First failure - Fatigue failure in leading edge of airfoil 3.25 inches above base platform after 450 hours at rated speed. Note depletion zone and oxide penetrations along leading edge. X100.



Third last failure - Stress-rupture failure after 848 hours at rated speed $2 \frac{3}{16}$ inches above base and $\frac{5}{8}$ inch in from leading edge.

Note intergranular nature of failure. (Last two blades failed by fatigue at 857.5 hours at rated speed.) X100.



Failure origin of above specimen at X750.



Section of failure-origin area showing intergranular nature of failure propagation. X750.

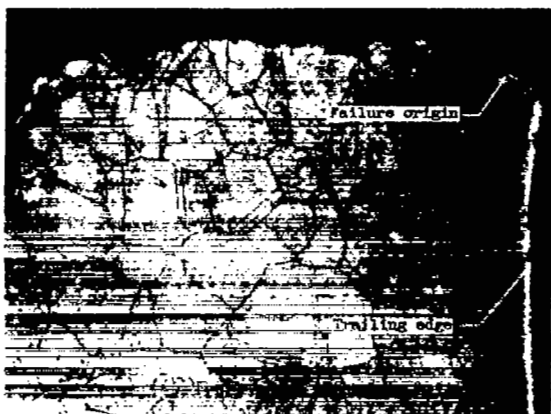
C-38976

(a) Group 1.

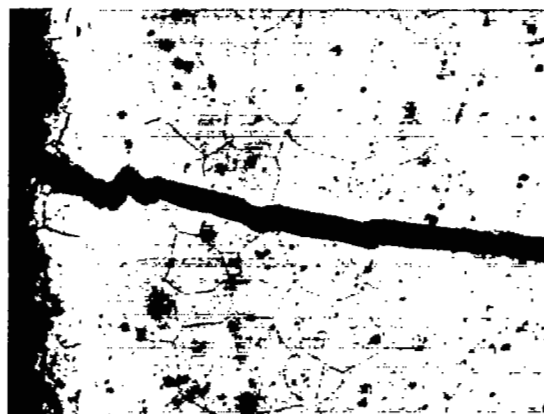
Figure 10. - Microstructures of failure origins of first and last failed Inconel 550 blades operated in engine under cyclic operating conditions. Etchant: 5 cc HF, 20 cc glycerine, 20 cc water; electrolytic.

3562

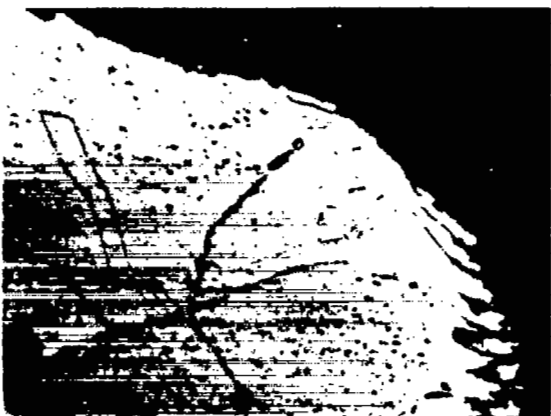
CL-6 back



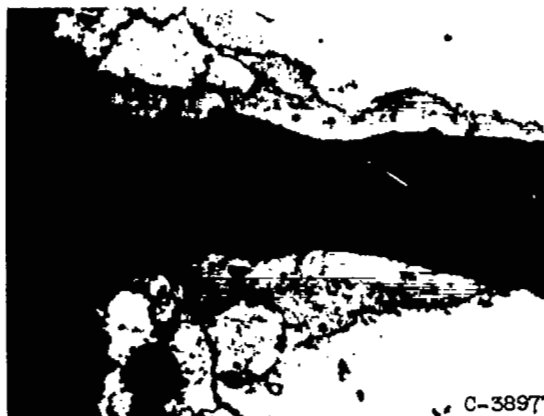
Second failure - Fatigue failure occurring in trailing edge $3\frac{1}{32}$ inches above base platform after 277.6 hours at rated speed. Note depletion zone and penetration of grain boundary. (Specimen of first failure lost; failure occurred by fatigue after 186 hr at rated speed.) X100.



Last failure - Fatigue failure occurring in leading edge $3\frac{3}{32}$ inches above base platform after 788 hours at rated speed. Note depth of depletion zone and excessive oxide generation of trailing edge. X100.



Failure origin of above specimen at X750. Note oxide penetration of depletion zone and indications of fatigue at failure origin.



Failure origin of above at X750. Note thickness of oxide on failure face which indicates that separation occurred appreciably before blade was considered failed.

(b) Group 2.

Figure 10. - Continued. Microstructures of failure origins of first and last failed Inconel 550 blades operated in engine under cyclic operating conditions. Etchant: 5 cc HF, 20 cc glycerine, 20 cc water; electrolytic.



First failure - Fatigue failure occurring in leading edge $2\frac{15}{16}$ inches above base platform after 235 hours at rated speed. Note depletion zone and oxide penetrations along leading edge. X100.



Last failure - Failure occurring by stress-rupture plus fatigue in leading edge $3\frac{1}{32}$ inches above base platform after 540 hours at rated speed. Note recrystallization in depletion zone, oxide penetrations and stress-rupture tearing present in failure area. X100.



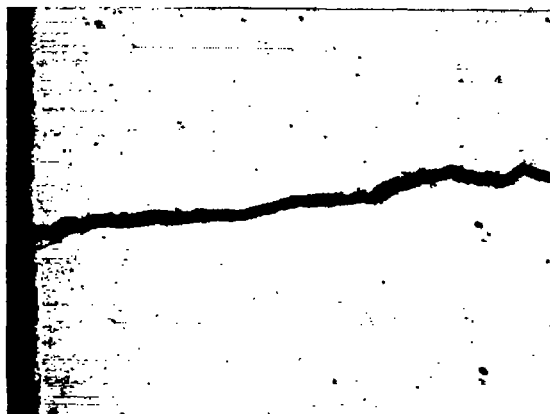
Failure origin of above specimen at X750. Note oxide penetration of grain boundary and presence of recrystallized grains in depletion zone.



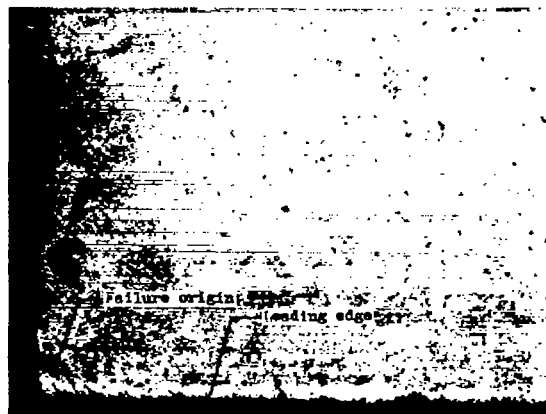
Failure origin of above specimen at X750.

(c) Group 3.

Figure 10. - Continued. Microstructures of failure origins of first and last failed Inconel 550 blades operated in engine under cyclic operating conditions. Etchant: 5 cc HF, 20 cc glycerine, 20 cc water; electrolytic.



First failure - Fatigue failure originating in leading edge 3 inches above base platform after 290 hours at rated speed. X100.



Last failure - Fatigue failure originating in leading edge $3\frac{3}{32}$ inches above base platform after 670 hours at rated speed. Note depletion zone and oxide penetration along leading edge. X100.



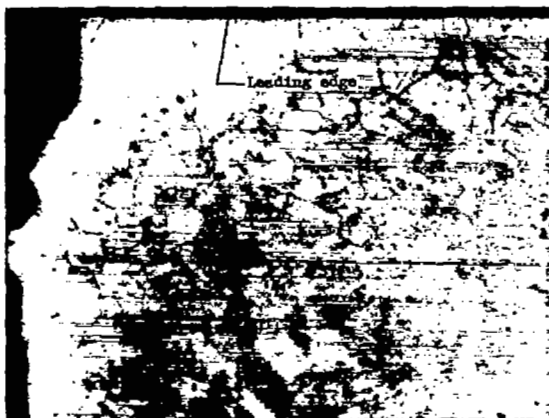
Failure origin of above specimen at X750. Note oxide penetrations and extent of depletion of leading edge and grain boundaries adjacent to failure path.



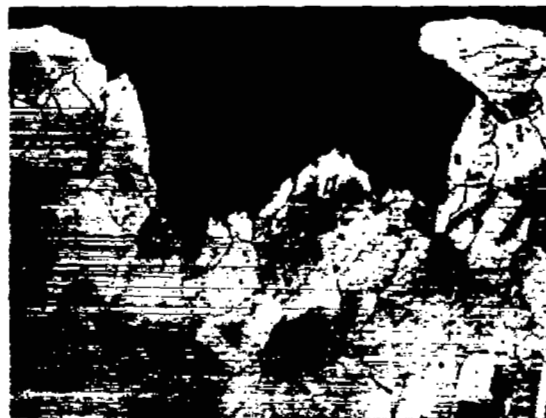
Failure origin of above specimen at X750. Note depletion zone in grain boundary in interior of specimen.

(d) Group 4.

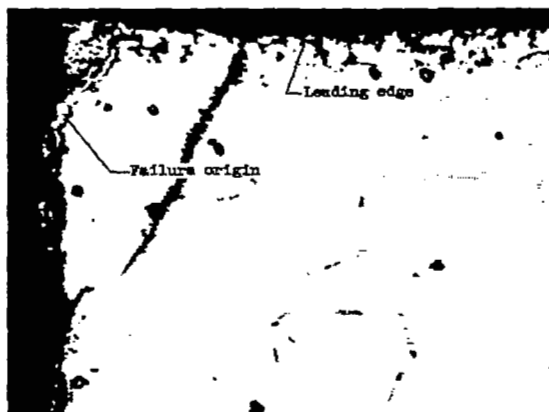
Figure 10. - Continued. Microstructures of failure origins of first and last failed Inconel 550 blades operated in engine under cyclic operating conditions. Etchant: 5 cc HF, 20 cc glycerine, 20 cc water; electrolytic.



First failure - Fatigue failure occurring in leading edge 3 inches above base platform after 416 hours at rated speed. Note heavy oxide on failure edge which indicated that separation occurred appreciably before blade failed. X100.



Last failure - Stress-rupture failure occurring $2\frac{7}{16}$ inches above base platform and towards center of blade chordwise. Note stress-rupture tearing below failure edge. X100.



Failure origin of above specimen at X750. Note recrystallization in depletion zone and extent of oxide penetration.



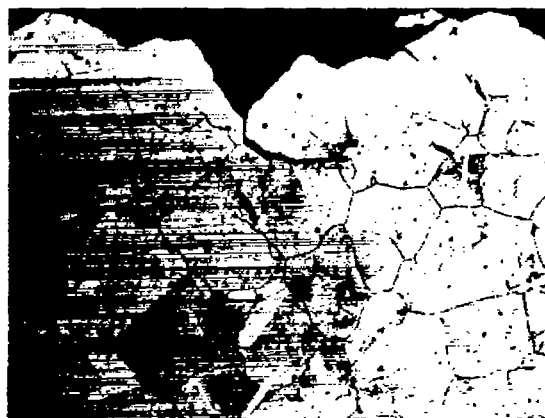
Section of above failure edge at X750 indicating intergranular nature of failure.

(e) Group 5.

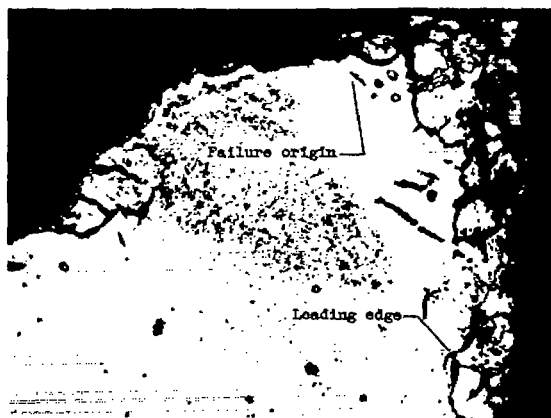
Figure 10. - Continued. Microstructures of failure origins of first and last failed Inconel 550 blades operated in engine under cyclic operating conditions. Etchant: 5 cc HF, 20 cc glycerine, 20 cc water; electrolytic.



First failure - Fatigue failure occurring in leading edge 3 inches above base platform after 278 hours at rated speed. Note depletion zone and oxide penetrations along leading edge. X100.



Last failure - Stress rupture failure occurring in leading edge $2\frac{3}{16}$ inches above base platform and $\frac{5}{8}$ inch in from edge. Note transgranular tearing below failure edge. Failure occurred after 747 hours at rated speed. X100.



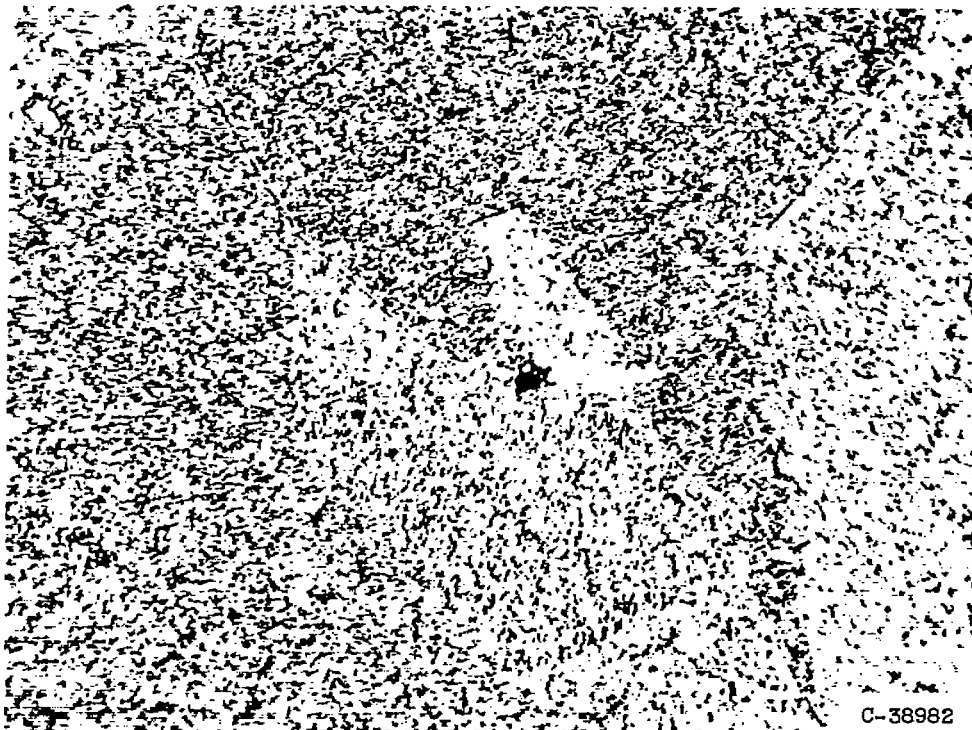
Failure origin of above specimen at X750.



Section of above failure edge at X750. Note oxide layer present on failure edge and intergranular nature of failure.

(f) Group 6.

Figure 10. - Concluded. Microstructures of failure origins of first and last failed Inconel 550 blades operated in engine under cyclic operating conditions. Etchant: 5 cc HF, 20 cc glycerine, 20 cc water; electrolytic.



C-38982

Figure 11. - Typical microstructure of Inconel 550 blades after engine operation. (Specimen taken from a group 6 blade which failed at 278 hr rated-speed operation.) Etchant: 5 cc HF, 20 cc glycerine, 20 cc water; electrolytic. X750.

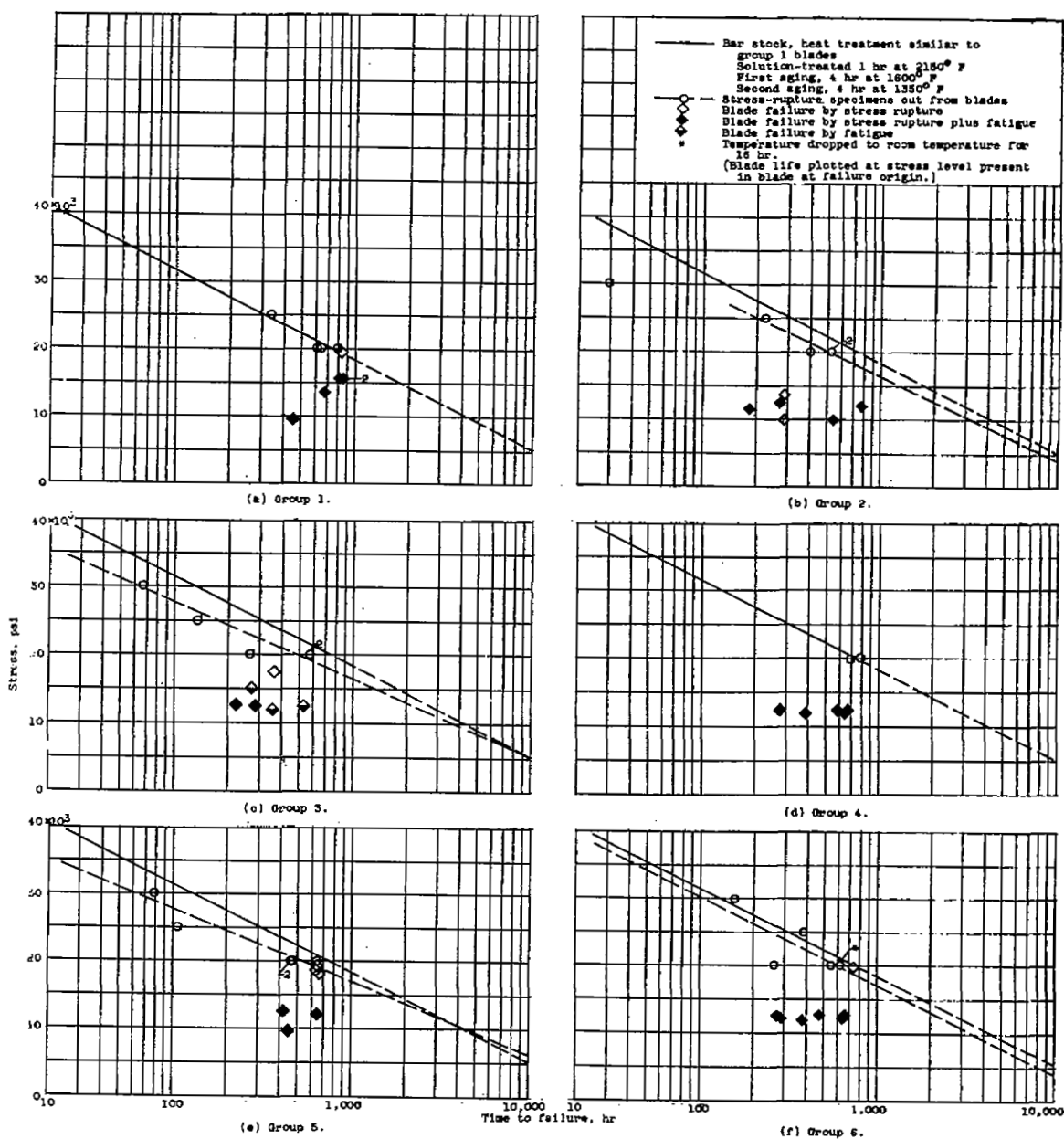


Figure 12. - Comparison of blade life and stress-rupture life of bar stock and specimens cut from blades at 1500° F test temperature.

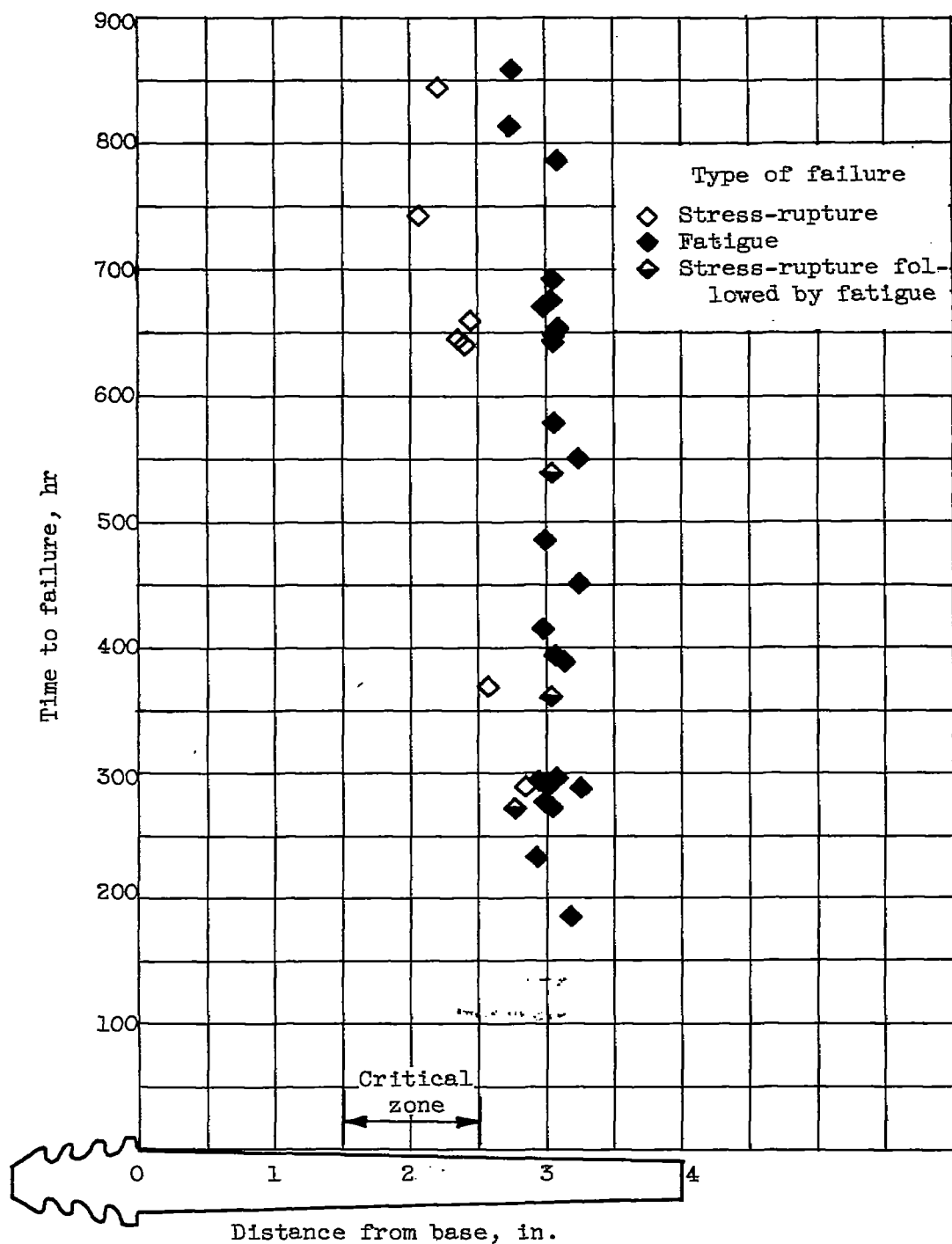


Figure 13. - Occurrence of failures in Inconel 550 with respect to blade length. Damage failures excluded.

NASA Technical Library



3 1176 01435 4972

